

# Crystal Structure and Magnetism of Actinide Oxides: A Review

Binod K. Rai,<sup>1,\*</sup> Alex Breña,<sup>1</sup> Gregory Morrison,<sup>2</sup> Ryan Greer,<sup>1</sup> Krzysztof Gofryk,<sup>3,4</sup> and Hans-Conrad zur Loye<sup>2</sup>

<sup>1</sup>*Savannah River National Laboratory, Aiken, SC, 29808 USA*

<sup>2</sup>*Department of Chemistry and Biochemistry, University of South Carolina, 631 Sumter Street, Columbia, SC, USA*

<sup>3</sup>*Idaho National Laboratory, Idaho Falls, Idaho 83402 USA*

<sup>4</sup>*Glenn T. Seaborg Institute, Idaho National Laboratory, Idaho Falls, Idaho 83402 USA*

(Dated: March 5, 2024)

In actinide systems, the 5f electrons experience a uniquely delicate balance of effects and interactions having similar energy scales, which are often difficult to properly disentangle. This interplay of factors such as the dual nature of 5f-states, strong electronic correlations, and strong spin-orbit coupling results in electronically unusual and intriguing behavior such as multi-k antiferromagnetic ordering, multipolar ordering, mott-physics, mixed valence configurations, and more. Despite the inherent allure of their exotic properties, the exploratory science of even the more basic, binary systems like the actinide oxides has been limited due to their toxicity, radioactivity, and reactivity. In this article, we provide an overview of the available synthesis techniques for selected binary actinide oxides, including the actinide dioxides, sesquioxides, and a selection of higher oxides. For these oxides, we also review and evaluate the current state of knowledge of their crystal structures and magnetic properties. In many aspects, substantial knowledge gaps exist in the current body of research on actinide oxides related to understanding their electronic ground states. Bridging these gaps is vital for improving not only a fundamental understanding of these systems but also of future nuclear technologies. To this end, we note the experimental techniques and necessary future investigations which may aid in better elucidating the nature of these fascinating systems.

## ABBREVIATIONS

### I. GLOSSARY OF ACRONYMS

*fcc*: Face-Centered Cubic

*bcc*: Body-Centered Cubic

AFM: Antiferromagnetic

FM: Ferromagnetic

$T_N$ : Néel temperature

$T_0$ : Transition temperature

mK: Milli-Kelvin

mg: Milli-gram

$\mu$ g: Micro-gram

JT: Jahn–Teller

DFT: Density Functional Theory

INS: Inelastic Neutron Scattering

NMR: Nuclear Magnetic Resonance

XPS: X-ray Photoelectron Spectroscopy

$\mu$ SR: Muon Spin Relaxation

### II. INTRODUCTION

The consequences of 5f electrons in the actinide elements are as interesting as they are complex, with actinide systems displaying dual nature of 5f states (itinerant-localized), competing interactions, and strong spin-orbit coupling[1–4]. Actinide materials can have both local and itinerant moment character due to their

partially filled 5f shells[5], effects which can exhibit profound competition in actinide compounds. This interplay results in unusual behavior from a magnetism perspective, such as hidden order[1, 6–13], complex magnetic order[14–16], topological phenomena[17, 18], mixed valence configurations[19–22], changes in covalency[23–25], and Mott transitions[2, 18, 26]. Such dual moment nature and large spin-orbit coupling observed in actinide materials contribute to their diverse physical and chemical properties, and therefore, a better understanding of these properties has the potential to advance fundamental actinide science as well as the future of energy and information technology. However, the exploratory science of actinide materials has been extremely limited due to the toxicity, radioactivity, and reactivity of the actinide elements. Consequently, not all established approaches to sample synthesis can be employed, particularly when it comes to single crystals. In addition to challenges related to sample quality, the complexity of actinide oxides is further exacerbated by the absence of an accurate description of their electronic structure. This inaccuracy stems from intricate interactions, including strong electron correlations, crystal field interactions resulting from the electric field generated by surrounding ligands or ions, and coupled spin-orbit interactions that arise from relativistic effects, which intertwine an atom’s electron spin and orbital motion. These interactions profoundly impact the electronic structure, magnetic and spectroscopic properties of actinides, influencing their chemical reactivity and bonding patterns. A detailed description of these interactions is well discussed in references[1, 2, 27] and recent advancements in theoretical calculations and modeling which consider these interactions in actinide oxides are discussed here[20, 28–32].

\* binod.raai@srnl.doe.gov

Historically, the bulk of actinide oxide research has focused on the properties of various uranium and plutonium compounds as they impact their use in the nuclear fuel industry. While the fundamental understanding of compounds such as  $\text{UO}_2$  has improved, a fundamental grasp of the physical properties of other actinide oxides remains elusive. Several synthetic, structural and characterization challenges have impeded a better understanding of the actinide oxides: (i) a dearth of high-quality polycrystalline samples or single crystals, (ii) conflicting crystal structures of the higher actinide oxides, such as  $\text{Pa}_2\text{O}_5$ , (iii) a severe lack of experimental characterization of many actinide oxides, such as  $\text{Cm}_2\text{O}_3$ , and (iv) inconsistent and sometimes contradictory experimental magnetic properties, as observed in  $\text{NpO}_2$  and  $\text{AmO}_2$ .

Synthesizing high-quality samples of the higher actinide oxides, especially as single crystals, has been challenging due to the coexistence of different oxides with different oxidation states, as well as the inherent difficulties in handling the toxic, radioactive, and reactive actinide elements. This lack of high-quality samples has limited the determination of exact crystal structures of many higher actinide oxides. While the actinide dioxides crystallize in the simple face-centered cubic (*fcc*) fluorite structure, the sesquioxides and the higher oxides have more complicated crystal structures and can even crystallize in several polymorphic structures. Inadequate crystal quality, along with factors such as the inability of facilities to handle analytically amenable quantities of material and the lack of access to necessary experimental and analytical techniques have drastically impacted investigations into the electronic and magnetic properties, and has made determination of magnetic ground states an enduring problem in actinide materials. This is exemplified in compounds such as  $\text{AmO}_2$ ,  $\text{CmO}_2$ ,  $\text{U}_2\text{O}_5$ , and  $\text{U}_3\text{O}_7$ , whose ground states are still unresolved due to a lack of high-quality samples. Mössbauer spectroscopy[33] and neutron diffraction measurements have failed to detect any magnetic order below the transition temperature  $T_0 = 8.5$  K in  $\text{AmO}_2$ [34]. However, recent Nuclear Magnetic Resonance (NMR) measurements on  $\text{AmO}_2$  performed by *Tokunaga et al.*[14, 15] confirmed the phase transition seen at  $T_0$ . Magnetic characterizations of higher actinide oxides like  $\text{U}_2\text{O}_5$ ,  $\text{U}_3\text{O}_7$ , and  $\text{Pa}_2\text{O}_5$  have yet to be explored. To overview such recent discoveries and uncover the potential of unexplored actinide oxides, there is a need for a review article that summarizes the behavior of actinide oxides.

In this article, we summarize the main challenges in actinide oxide synthesis together with their magnetic properties and the scientific potential of unexplored actinide

oxides. More comprehensive reviews on actinide metals, intermetallic actinide materials, and thin film actinide oxide materials have been covered elsewhere[35–41]. It is not our intention to cover any specialized techniques that have been discussed in detail in other articles, such as NMR[42, 43], Synchrotron Radiation[44], Density Functional Theory (DFT)[45], or X-ray Photoelectron Spectroscopy (XPS)[46]. For most bulk binary actinide oxides, we cover their crystal growth methods in Section III, the current state of our understanding of their magnetic properties in Section IV, and summary and recommendations for future work in Section V.

### III. CRYSTAL GROWTH

Actinides are generally difficult to handle due to their scarcity, reactivity, radioactivity, and toxicity. Light elements, such as Th and U, can be handled in kilogram quantities, but heavier elements are typically limited to *mg* or even  $\mu\text{g}$  sample sizes due to their high activity. Given these limitations, work on actinide materials synthesis is limited, and only very few specialized laboratories across the globe are able to undertake such experiments. Several reviews of the synthesis of binary actinide oxides exist[47–49]. We have attempted to give an overview of all the synthesis techniques including those developed since the last review over 15 years ago in Table I, along with the corresponding references. A brief description of these methods with selected references is provided below. Structural information for each compound is provided in Table II and III. The lattice parameters reported are at room temperature unless otherwise stated in the text.

Polycrystalline samples of actinide oxides are most commonly synthesized by calcination of various precursors including the oxalates[50, 51] nitrates[52] and hydroxides[53]. Controlling the atmosphere during calcination, or post-synthetic oxidation/reduction, allows for control over the specific actinide oxide produced. For example, curium oxides were synthesized by the calcination of curium oxalate.  $\text{Cm(III)}$  was precipitated from a 0.1 M HCl solution with oxalate ions. The resulting curium oxalate was calcined in oxygen at 1000 °C, resulting in an intermediate oxygen stoichiometry. This product was then heated at 1100 °C in vacuum or carbon monoxide to produce  $\text{Cm}_2\text{O}_3$ , or at lower temperatures in 4 – 5 atm of oxygen to produce  $\text{CmO}_2$ [51]. For smaller scale,  $\mu\text{g}$  reactions, calcination of ion-exchange resins is also possible[54]. Synthesis of polycrystalline samples of actinide oxides have also been reported through sol-gel[55] and aqueous routes[56–58].

TABLE I: GROWTH METHODS

Compound	Synthesis Method	Form	References
$\text{ThO}_2$	Calcination of oxalate - air	Powder	[50, 59]
	Sol-gel	Powder	[55, 60]
	From melt	Single Crystal	[61]
	Flux - Lead and other flux	Single Crystal	[62–68]

TABLE I – Continued from previous page

Compound	Synthesis Method	Form	References
	Hydrothermal	Single Crystal	[69, 70]
	Sublimation/deposition	Single Crystal	[71]
	Electrodeposition from plasma	Single Crystal	[72, 73]
PaO <sub>2</sub>	Reduction of oxide hydrate - H <sub>2</sub>	Single Crystal	[74]
Pa <sub>2</sub> O <sub>5</sub>	Calcination of various Pa compounds - air/O <sub>2</sub>	Powder	[75]
	Dehydration of oxide hydrate	Powder	[74, 76]
	Precipitation of molten salt - HF/H <sub>2</sub> O purge	Powder	[77]
UO <sub>2</sub>	Sol-gel	Powder	[55]
	Reduction of U <sub>3</sub> O <sub>8</sub> or UO <sub>3</sub>	Powder	[78]
	Aqueous	Powder	[56]
	From melt	Single Crystal	[61, 79, 80]
	Floating Zone	Single Crystal	[81]
	Flux growth - UCl <sub>4</sub>	Single Crystal	[82]
	Electrodeposition - chloride melt	Single Crystal	[83–85]
	Hydrothermal	Single Crystal	[86–88]
	Vapor Transport - chloride species or others	Single Crystal	[89–92]
	Sublimation	Single Crystal	[85, 93]
	Electrodeposition from plasma	Single Crystal	[73]
U <sub>4</sub> O <sub>9</sub>	Comproportionation of UO <sub>2</sub> and U <sub>3</sub> O <sub>8</sub>	Powder	[94, 95]
	Oxidation of UO <sub>2</sub>	Single Crystal or Powder	[96–101]
	Electrodeposition - chloride melt	Single Crystal	[83]
	Vapor transport - HCl or Cl <sub>2</sub>	Single Crystal	[89]
U <sub>3</sub> O <sub>7</sub>	Oxidation of UO <sub>2</sub>	Powder	[97]
$\beta$ -U <sub>3</sub> O <sub>7</sub>	Oxidation of UO <sub>2</sub>	Powder	[98, 100, 102–104]
U <sub>2</sub> O <sub>5</sub>	Comproportionation of UO <sub>2</sub> and U <sub>3</sub> O <sub>8</sub> - High P	Powder	[105]
	Reduction of U <sub>3</sub> O <sub>8</sub> - single crystals	Single Crystal	[106]
	Decomposition of UO <sub>2</sub> Cl <sub>2</sub>	Single Crystal	[107]
$\alpha$ -U <sub>3</sub> O <sub>8</sub>	Calcination of oxalate or nitrate - air/He/O <sub>2</sub>	Powder	[52, 108]
	UO <sub>2</sub> Oxidation	Powder	[109, 110]
	UO <sub>3</sub> Reduction	Powder	[111]
	Vapor Transport - HCL	Single Crystal	[89]
	UO <sub>2</sub> Cl <sub>2</sub> decomposition	Single Crystal	[112]
$\beta$ -U <sub>3</sub> O <sub>8</sub>	Heat treating $\alpha$ -U <sub>3</sub> O <sub>8</sub>	Powder	[113]
	Sublimation/Deposition	Single Crystal	[114]
$\alpha$ -UO <sub>3</sub>	Crystallization of amorphous UO <sub>3</sub> - High pressure O <sub>2</sub>	Powder	[83]
	Dehydration of H <sub>2</sub> U <sub>3</sub> O <sub>10</sub>	Powder	[115]
	Calcination of UO <sub>4</sub> 2H <sub>2</sub> O or NH <sub>4</sub> UO <sub>2</sub> (NO <sub>3</sub> ) <sub>3</sub> - air or others	Powder	[116–119]
	Oxidation of U <sub>3</sub> O <sub>8</sub> - High pressure O <sub>2</sub>	Powder	[120]
$\beta$ -UO <sub>3</sub>	Calcination of nitrate or NH <sub>4</sub> UO <sub>2</sub> (NO <sub>3</sub> ) <sub>3</sub> - air or others	Powder	[118, 121, 122]
	Oxidation of U <sub>3</sub> O <sub>8</sub>	Powder	[120]
$\gamma$ -UO <sub>3</sub>	Calcination or nitrate or (NH <sub>4</sub> ) <sub>2</sub> UO <sub>2</sub> (NO <sub>3</sub> ) <sub>4</sub> 2H <sub>2</sub> O - air or others	Powder	[116, 118, 123]
	Flux - ZnCl <sub>2</sub>	Single Crystal	[124]
$\delta$ -UO <sub>3</sub>	Dehydration of $\beta$ -UO <sub>3</sub> H <sub>2</sub> O	Powder	[100, 125, 126]
$\epsilon$ -UO <sub>3</sub>	Oxidation of U <sub>3</sub> O <sub>8</sub> - NO <sub>2</sub> /O <sub>2</sub> /O <sub>3</sub>	Powder	[100, 127, 128]
UO <sub>4</sub>	Aqueous	Powder	[57]
NpO <sub>2</sub>	Calcination of oxalate or other compounds	Powder	[53, 127, 129–132]
	Aqueous	Powder	[56, 58]
	Flux - Lead or LiMoO <sub>2</sub>	Single Crystal	[66, 133]
	Electrochemical - Cl melt	Single Crystal	[134]
	Vapor transport - TeCl <sub>4</sub>	Single Crystal	[92, 135, 136]
Np <sub>2</sub> O <sub>5</sub>	Calcination of various Np compounds - air/vacuum	Powder	[130, 132, 137]
	Flux - LiClO <sub>4</sub>	Powder	[138, 139]
	Aqueous	Powder	[140]
	Mild hydrothermal	Single Crystal	[141]
Pu <sub>2</sub> O <sub>3</sub>	Reduction of PuO <sub>2</sub> - H <sub>2</sub> or C	Powder	[142, 143]
PuO <sub>2</sub>	Calcination of various Pu compounds - air	Powder	[132, 144]
	Oxygenation of PuF–4 - H <sub>2</sub> O	Powder	[145]
	Sol-gel	Powder	[55, 146, 147]
	Aqueous	Powder	[56]

TABLE I – *Continued from previous page*

Compound	Synthesis Method	Form	References
	Flux -various	Single Crystal	[66, 148–150]
	Vapor transport - $\text{TeCl}_4$	Single Crystal	[151]
	Precipitation from silicate glass	Single Crystal	[152]
$\text{Am}_2\text{O}_3$	Reduction of $\text{AmO}_2$ - $\text{H}_2$	Powder	[153–155]
$\text{AmO}_2$	Calcination of oxalate - air/ $\text{O}_2$	Powder	[131, 153, 154, 156, 157]
	Calcination of exchange resin - $\text{O}_2$	Powder	[155]
$\text{Cm}_2\text{O}_3$	Calcination of oxalate - $\text{CO}$ /vacuum	Powder	[51]
	Calcination of exchange resin - air	Powder	[158]
	Reduction of $\text{CmO}_2$ - $\text{H}_2/\text{Ar}_2$ /vacuum	Powder	[159–161]
$\text{CmO}_2$	Calcination of oxalate or nitrate - $\text{O}_2$ or $\text{O}_2$ - $\text{O}_3$ mixture	Powder	[51, 160, 162]
	Calcination of exchange resin - $\text{O}_2$	Powder	[163, 164]
	Oxidation of $\text{Cm}_2\text{O}_3$ - $\text{O}_2$	Powder	[165]
$\text{BkO}_2$	Calcination of oxalate - air/ $\text{O}_2$	Powder	[51, 131, 166]
	Calcination of exchange resin	Powder	[167, 168]
$\text{Cf}_2\text{O}_3$	Calcination of exchange resin - air	Powder	[169]
	Reduction of $\text{CfO}_2$ - $\text{H}_2$	Powder	[170]
$\text{CfO}_2$	Calcination of exchange resin - $\text{O}_2$	Powder	[169]

Many of the actinide oxides can be hypo- or hyperstoichiometric, i.e. containing less or more oxygen than the integer stoichiometry would imply. These require specific synthesis conditions or post-synthetic treatments to achieve stoichiometric products. Hypo- or hyperstoichiometry has been extensively studied in the uranium oxides. For example, highly variable stoichiometry exists between  $\text{UO}_2$  and  $\text{U}_3\text{O}_8$ . This includes several distinct stoichiometries, such as  $\text{U}_4\text{O}_9$ ,  $\text{U}_3\text{O}_7$ , and  $\text{U}_2\text{O}_5$ . Careful control of the oxidation of  $\text{UO}_2$ [94, 97, 99, 100] or reduction of  $\text{U}_3\text{O}_8$ [106] allows for the synthesis of these various compounds. For example,  $\text{U}_4\text{O}_9$  can be synthesized by the comproportionation of  $\text{UO}_2$  and  $\text{U}_3\text{O}_8$ [94]. It can also be synthesized by the oxidation of powder or single crystalline samples of  $\text{UO}_2$  using either a low oxygen concentration[97] or an adjacent  $\text{U}_3\text{O}_8$  sample, which releases oxygen upon heating, in a sealed system[99]. McEachern and Taylor provided a thorough review of the oxidation behavior of uranium dioxide[171].

In contrast to polycrystalline samples, single crystals offer the highest-quality specimens and enable the measurement of anisotropic properties, which are crucial for determining their often intricate magnetic characteristics. Techniques such as neutron scattering, resonant X-ray scattering, electronic and heat transport, and specific heat measurements become invaluable tools in this regard. Actinide materials exhibit complex magnetic behavior due to strong electronic correlations, spin-orbit coupling, and crystal-field interactions, underscoring the importance of precise and comprehensive characterization. However, achieving single crystal growth of actinide oxides presents an added layer of complexity in material preparation and handling, especially when compared to non-radioactive substances. For instance, when working with reactive, radioactive, and toxic elements, it is typically necessary to seal the materials in a quartz tube during crystal growth. One notable advantage of single crystals is that, in many instances, they require a significantly smaller quantity of material compared to poly-

crystalline samples for magnetic characterization, such as magnetic susceptibility and specific heat measurements, as well as neutron diffraction. Moreover, single crystals are the preferred choice when working with actinide materials for measurements, as polycrystalline powder materials have a higher potential for contamination.

The crystal growth of actinide oxides is made even more challenging by their very high melting points, their proclivity for auto-reduction at high temperatures, and their high inertness, especially of the dioxides. For instance,  $\text{ThO}_2$  has the highest melting point of any known binary oxides reaching up to 3,300 ° [172]. Despite their high melting points, single crystals of  $\text{ThO}_2$  and  $\text{UO}_2$  have been synthesized from their melts using synthesis methods that allow for extremely high temperatures, such as solar furnaces[80], electric arc furnaces[173], and RF furnaces[61]. Single crystals of  $\text{UO}_2$  have also been achieved using a floating zone furnace[81].

The difficulties of direct melt growth of actinide oxides make crystal growth techniques that can provide single crystal samples at more moderate temperatures very desirable[174–176]. Flux crystal growth[177] has been reported for  $\text{AcO}_2$  ( $\text{Ac} = \text{Th}, \text{U}, \text{Np}, \text{Pu}$ ). Lead containing fluxes, namely  $\text{PbF}_2$ ,  $\text{PbO}$ , and lead vanadate[63, 66] are the most commonly used, but other fluxes including lithium tungstate,  $\text{NaBO}_2$ , and  $\text{MoO}_2$  have also been reported[62, 67, 148]. In addition to flux growth, where precipitation is typically driven by cooling or evaporation of the flux, electrochemical crystal growth from chloride melts has been reported for  $\text{UO}_2$  and  $\text{NpO}_2$ [84, 134].

Along with using molten salts as a solvent, recent years have seen a number of developments in the use of hydrothermal synthesis wherein supercritical water is the solvent[141, 178] to grow crystals of  $\text{ThO}_2$  and  $\text{UO}_2$ [69, 86]. For example, large single crystals of  $\text{ThO}_2$ , up to several *mm* per side, were grown across a temperature gradient from seed crystals at 710 °C using polycrystalline  $\text{ThO}_2$  as a source material in 6 M  $\text{CsF}$  at 750 °C[69]. Mild hydrothermal synthesis[179], which oc-

curs in the temperature range above the boiling point of water but below the supercritical point, and aqueous routes[56, 180], which occur below the boiling point of water, have also been reported for some of the actinide oxides, but have only resulted in polycrystalline samples[56] or nanoparticles[179, 180].

A final, commonly reported growth method for the synthesis of single crystals is vapor transport[181], a method in which a polycrystalline material or precursor mixture is transported across a temperature gradient by a transport gas and redeposited as single crystals. Vapor transport has been reported for  $\text{NpO}_2$ ,  $\text{PuO}_2$  and several of the uranium oxides[89, 92, 151]. A chloride containing species, namely  $\text{HCl}$ ,  $\text{Cl}_2$ , or  $\text{TeCl}_4$ , is the most common transport agent.  $\text{ThO}_2$  has been grown by the direct sublimation/deposition of polycrystalline  $\text{ThO}_2$  without the use of a transport gas[71]. A graphical representation of synthesis methods is presented in Fig. ??.

As will be discussed in the Magnetic Properties section, achieving a better understanding of the behavior of

many of the binary actinide oxides necessitates further measurements, especially on single crystalline samples. The provided summary and Table I can serve as a guide for synthesizing such samples. For binary actinide oxides with only a limited number of synthesis procedures, especially where only polycrystalline products are obtained, the synthesis methods of other actinides, with proper consideration of oxidation states, can guide the development of suitable routes for synthesis. For later actinides particularly, issues both of supply and high radioactivity limit the amount of material available, complicating synthesis. For such species, hydrothermal synthesis has been shown to be scalable down to very small sample reaction masses,[182–185] using as little as  $< 1$  mg of actinide[185]. Recently, we have shown that flux growth can also be scaled down to the mg scale or even 1 mg scale[186, 187]. This suggests that these two synthesis techniques are likely suitable for the synthesis of many of the binary actinide oxides whose complete magnetic characterization necessitates single crystalline samples.

TABLE II: Crystal structure information of Actinide Oxides

Compound	Crystal Symmetry	Space Group	Lattice Parameters(Å)				References
			a	b	c	$\beta$	
$\text{ThO}_2$	Cubic	$\text{Fm}\bar{3}\text{m}$	5.597				[188]
$\text{PaO}_2$	Cubic	$\text{Fm}\bar{3}\text{m}$	5.505				[74]
$\text{Pa}_2\text{O}_3$	Cubic	$\text{Fm}\bar{3}\text{m}$	5.505				[74]
$\text{NpO}_2$	Cubic	$\text{Fm}\bar{3}\text{m}$	5.434				[188]
$\text{Np}_2\text{O}_5$	Monoclinic	$\text{P}2_1/\text{c}$	8.168	6.584	9.313	116.09	[141]
$\text{PuO}_2$	Cubic	$\text{Fm}\bar{3}\text{m}$	5.395				[188]
$\alpha\text{-Pu}_2\text{O}_3$	Cubic	$\text{Ia}\bar{3}$	11.04				[189]
$\alpha'\text{-Pu}_2\text{O}_3$	Cubic	$\text{Ia}\bar{3}$	5.409				[189]
$\beta\text{-Pu}_2\text{O}_3$	Hexagonal	$\text{P}6_3/\text{mmc}$	3.841	3.841	5.958		[189]
$\text{AmO}_2$	Cubic	$\text{Fm}\bar{3}\text{m}$	5.139				[190]
$\text{Am}_2\text{O}_3$	Monoclinic	$\text{C}2/\text{m}$	14.315	3.6793	8.9271	100.37	[191, 192]
	Hexagonal	$\text{P}\bar{3}\text{m}1$	3.8123	3.8123	5.9845		[155, 191, 192]
	Cubic	$\text{Ia}\bar{3}$	11.012				[155, 191, 192]
$\text{CmO}_2$	Cubic	$\text{Fm}\bar{3}\text{m}$	5.358				[51, 190, 193]
$\text{Cm}_2\text{O}_3$	Monoclinic	$\text{C}2/\text{m}$	14.282	3.652	8.900	100.31	[51, 194]
	Hexagonal	$\text{P}\bar{3}\text{m}1$	3.80	3.80	6.00		[51]
$\text{BkO}_2$	Cubic	$\text{Ia}\bar{3}$	10.97				[195]
	Cubic	$\text{Fm}\bar{3}\text{m}$	5.333				[51, 196]
$\text{Bk}_2\text{O}_3$	Cubic	$\text{Ia}\bar{3}$	10.887				[196]
	Monoclinic	$\text{C}2/\text{m}$	14.197	3.606	8.846	100.23	[54]
$\text{CfO}_2$	Cubic	$\text{Fm}\bar{3}\text{m}$	5.310				[169]
$\text{Cf}_2\text{O}_3$	Cubic	$\text{Fm}\bar{3}\text{m}$	10.809				[169, 197, 198]
	Monoclinic	$\text{C}2/\text{m}$	14.124	3.591	8.809	100.31	[197, 199]

\* = Magnetic properties and the magnetic ground state have not been studied in detail or remain unresolved

TABLE III: Crystal structure information of Uranium Oxides

Compound	Crystal Symmetry	Space Group	Lattice Parameters(Å)				References
			a	b	c	$\beta$	
$\text{UO}_2$	Cubic	$\text{Fm}\bar{3}\text{m}$	5.47	5.47	5.47		[188, 200, 201]
$\alpha\text{-UO}_3$	Orthorhombic	$\text{C}2\text{mm}$	3.913	6.936	4.167		[202, 203]
		$\text{C}222$	6.84	43.45	4.157		[117]
$\beta\text{-UO}_3$	Monoclinic	$\text{P}2_1/\text{m}$	10.34	14.33	3.910	99.03	[121, 203]
$\gamma\text{-UO}_3$	Orthorhombic	$\text{F}_{ddd}$	9.79	19.93	9.71		[204]
		$\text{I}4_1$	6.90	6.90	19.98		[204]
$\delta\text{-UO}_3$	Cubic	$\text{Pm}\bar{3}\text{m}$	4.165	4.165	4.165		[126]
$\eta\text{-UO}_3$	Orthorhombic	$\text{P}2_12_12_1$	7.51	5.47	5.22		[205]

TABLE III – *Continued from previous page*

Compound	Crystal Symmetry	Space Group	Lattice Parameters(Å)				References
			a	b	c	$\beta$	
$\alpha$ -U <sub>3</sub> O <sub>8</sub>	Orthorhombic	Amm2	6.716	11.960	4.147		[110, 202, 206]
	Hexagonal	P62m	6.812	6.812	4.142	120	[110]
$\beta$ -U <sub>3</sub> O <sub>8</sub>	Orthorhombic	Cmcm	7.069	11.445	8.303		[110, 113]
U <sub>3</sub> O <sub>7</sub>	Cubic	P4 <sub>2</sub> /nnm	5.3799	5.3799	5.5491		[207]
$\alpha$ -U <sub>2</sub> O <sub>5</sub>	Unk.	Unk.	Unk.	Unk.	Unk.	Unk.	[105, 208]
$\beta$ -U <sub>2</sub> O <sub>5</sub>	Hexagonal	Unk.	3.813	3.813	13.180		[105]
$\gamma$ -U <sub>2</sub> O <sub>5</sub>	Monoclinic	Unk.	5.410	5.481	5.410	90.49	[105]
$\delta$ -U <sub>2</sub> O <sub>5</sub>	Orthorhombic	Pnma	6.849	8.274	31.706		[208]
$\alpha$ -U <sub>4</sub> O <sub>9</sub>	Cubic	R3c	18.9286	18.9286	18.9286		[98, 209]
$\beta$ -U <sub>4</sub> O <sub>9</sub>	Cubic	I43d	21.766	21.766	21.766		[98]
$\gamma$ -U <sub>4</sub> O <sub>9</sub>	Cubic	I43d	21.944	21.944	21.944		[21]

Note: The magnetic properties and magnetic ground state of the above uranium oxides, except for UO<sub>2</sub> and U<sub>3</sub>O<sub>8</sub>, have not been studied in detail or remain unresolved

#### IV. MAGNETIC PROPERTIES

The magnetism of binary actinide oxides through californium are discussed. The oxidation states of these actinides within these compounds are complex. If these actinide compounds follow the same magnetic systematics as the lanthanide compounds and, assuming the ground state is defined by Hund's-rule and  $L - S$  coupling ( $L$  being the total orbital angular momentum,  $S$  being the total spin angular momentum), the ionic-like compounds which correspond to  $5f$  electronic configurations should have finite paramagnetic effective moments, with the exceptions of the  $5f^4$  (singlet ground state) and  $5f^6$  ( $J=0$ ) states that lead to a theoretical moment of  $0 \mu_B$ . For example, Am<sub>2</sub>O<sub>3</sub> and CmO<sub>2</sub> should be ionic-like compounds corresponding to the  $5f^6$  electronic configuration and therefore, should have theoretical values of  $0 \mu_B$  for their paramagnetic effective moment. Cm<sub>2</sub>O<sub>3</sub> and BkO<sub>2</sub> should be ionic-like compounds corresponding to the  $5f^7$  configuration, with  $J = S = \frac{7}{2}$  ( $J$  being the total angular momentum), and an expected effective moment of  $7.94 \mu_B$ . However,  $L - S$  coupling may not be the most appropriate scheme for describing the ground-state wave functions in heavy actinides due to the large spin-orbit coupling and significant mixing of Hund's rule ground states by other  $LS$  states with the same  $J$  value. Thus, an intermediate coupling model between  $L - S$  and  $j-j$  coupling may be necessary[51]. The magnetic ordering temperatures and effective moments of actinide oxides through californium are shown in Fig. 1. Magnetic susceptibilities of various binary actinide oxides are presented in Fig. 2 and 3.

In general, in the  $5f$ -electron materials with strong spin-orbit coupling, dipole moments (the first term of a multipolar expansion) are insufficient to explain the observed phase transitions or quantum phenomena and, therefore, higher terms of the multipolar expansion are required. For example, multipolar ordering in NpO<sub>2</sub> arises at the atomic scale from strong spin-orbit coupling, which is difficult to detect because of the lack of response of high-rank multipoles to external perturbations. In other words, the characterization of the anisotropic dis-

tributions of electric and magnetic charges around given points of the crystal structure is challenging. Similar to NpO<sub>2</sub>, Mössbauer spectroscopy[33] and neutron diffraction measurements failed to detect any magnetic order below  $T_0 = 8.5$  K in AmO<sub>2</sub>[34]. However, NMR measurements on AmO<sub>2</sub> performed by *Tokunaga et al.*[14, 15] confirmed the phase transition seen at  $T_0$ , although the NMR spectrum of AmO<sub>2</sub> is rather different from that seen in the antiferromagnetic ground state of UO<sub>2</sub>[210] or the multipolar ground state of NpO<sub>2</sub>[211].

For some actinide oxides, their true magnetic ground state remains undetermined despite prior investigation of their magnetic properties. For example, PuO<sub>2</sub> shows a temperature independent magnetic susceptibility in between 4 – 1000 K [212] and NMR measurements have confirmed the absence of any magnetic order or structural distortions down to 6 K[213]. However, several theoretical studies[32, 214–216] have predicted an antiferromagnetic (AFM) ground state for PuO<sub>2</sub>. Based on the ionic picture, CmO<sub>2</sub> should have a singlet, nonmagnetic ground state and the magnetic susceptibility should behave as in PuO<sub>2</sub>. In actuality, the magnetic susceptibility of CmO<sub>2</sub> is temperature-dependent, shows a large effective moment of  $3.36(6) \mu_B$ [51, 193], and is suggested to have a mixed valence configuration of  $5f$  electrons[20].

While the antiferromagnetic structure in UO<sub>2</sub> (fluorite type, Fm $\bar{3}$ m s.g. crystal structure) was first reported by Frazer et al. in 1965[217], the internal distortion of oxygen atoms within the ordered state was discovered using high-quality single crystals in 1975[12]. More recently, it was shown that the dynamic Jahn-Teller distortion[218] (internal distortion) causes change in the space group from Fm $\bar{3}$ m to Pa $\bar{3}$ [1, 219]. This detailed crystal structure information, obtained from single crystals of UO<sub>2</sub>, has proven invaluable in comprehending both the complex magnetic structure and phonon dispersion. Such in-depth studies of other actinide oxides, particularly higher actinide oxides, have seldom (if ever) been explored experimentally, and their magnetic ground states often remain unresolved. For instance, no magnetic characterization, including thermodynamic measurements, has been conducted on oxides like U<sub>2</sub>O<sub>5</sub>, U<sub>3</sub>O<sub>7</sub> and Pa<sub>2</sub>O<sub>5</sub>. In

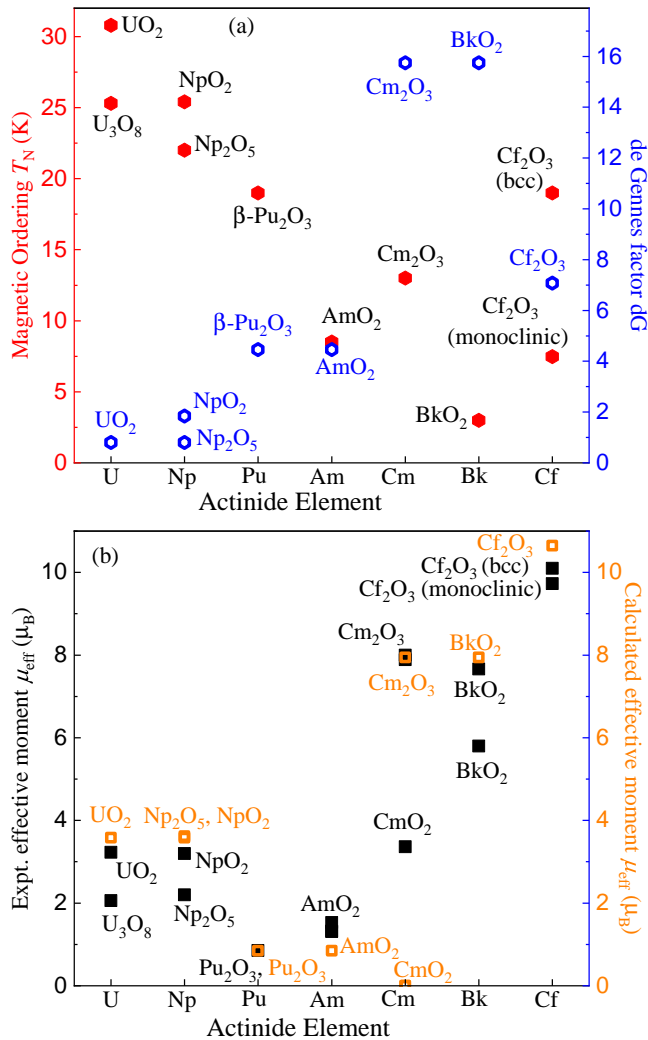


FIG. 1. (a) Magnetic ordering temperatures (left-axis) and de Gennes factor  $dG$  (right-axis) (b) experimental effective moments (left-axis) and theoretical effective moments (right-axis) of actinide elements:  $UO_2$  [220],  $U_3O_8$  [221, 222],  $U_4O_9$  [223],  $NpO_2$  [224],  $Np_2O_5$  [141],  $\beta$ - $Pu_2O_3$  [225],  $AmO_2$  [226],  $CmO_2$  [51, 193],  $Cm_2O_3$  [159],  $BkO_2$  [227],  $Cf_2O_3$  [170].

the following sections, we provide a review of the current magnetic properties reported for actinide dioxides in Sec. IV A, the actinide sesquioxides in Sec. IV B, and various selected higher oxides in Sec. IV C.

## A. Magnetic properties of actinide dioxides

### 1. Thorium Dioxide: $ThO_2$

Due to the stability of  $ThO_2$  and its importance in the nuclear technology, it is one of the most widely studied and well-characterized actinide dioxides.  $ThO_2$  is a diamagnetic insulator marked by a negative magnetic sus-

ceptibility ( $\chi = -16 \times 10^{-6} \text{ cm}^3/\text{mol}$  [228]) and a heat capacity that does not show any sign of phase transitions [229], as well as a band gap near 6 eV [230, 231]. Other physical properties have been well studied and are summarized by *Belle et al.* [232] and recently by *Hurley et al.* [41].  $ThO_2$  crystallizes in a fluorite-like face-centered cubic ( $fcc$ ) structure ( $Fm\bar{3}m$  Space Group [233]) with a lattice parameter of 5.597 Å [188]. It is worth mentioning that all actinide dioxides are isostructural, sharing the same fluorite  $fcc$  structure as that of  $ThO_2$  and therefore,  $ThO_2$  is often used as a matrix for studying the unique properties of the rarer transuranic elements. Under the pressure of 40 GPa,  $ThO_2$  undergoes a structural phase transition like other fluorite structures from cubic to a high-pressure orthorhombic structure ( $Pnma$  Space group, known as cotunnite) [234–236].

### 2. Uranium Dioxide: $UO_2$

$UO_2$  has been shown to be rather complex as compared to  $ThO_2$  due to the presence of 5f-electrons in its electronic configuration. A Mott-Hubbard insulator  $UO_2$  crystallizes in the shared fluorite cubic structure seen in  $ThO_2$  with a lattice parameter of 5.4731(4) Å and also displays the cotunnite orthorhombic structure at high pressure [200, 236–239]. In  $UO_2$ , uranium exhibits the 4+ oxidation state, yielding a  $5f^2$  configuration based on the ionic picture. An initial specific heat experiment hinted at a magnetic phase transition [240]. Shortly thereafter, neutron diffraction studies on  $UO_2$  single crystals determined a first-order AFM phase transition at  $T_N = 30.8 \text{ K}$  [217, 241]. After decades of research, the magnetic state below  $T_N$  was determined to be characterized by an antiferromagnetic non-collinear  $3-k$  structure [242–246] accompanied by Jahn-Teller (JT) distortions of the oxygen atoms in the  $fcc$  fluorite structure [1, 10–13].

Inelastic neutron scattering experiments first reported a possible strong coupling between the magnons and the crystal lattice in  $UO_2$  [247, 248]. The first-order nature of the phase transition at  $T_N$  arises from couplings between magnetic dipoles and electric quadrupoles ( $3-k$  type) [1, 8, 9] as marked by a sharp transition in various thermodynamic measurements such as magnetic susceptibility [249], heat capacity [250], thermal expansion, and elastic constants [11, 42, 43, 49, 249]. Subsequently, a dynamic JT distortion model was proposed to explain the strong magnetoelastic interactions seen well above  $T_N$  [243]. NMR studies [210] support the idea of a  $3-k$  magnetic structure in  $UO_2$  below  $T_N$  and provide strong evidence for local distortions as well as an excitation spectrum that shows the presence of magnon-phonon coupling. Many first principle studies have further explained and successfully modeled the non-coplanar  $3k$  magnetic structure below  $T_N$  [28, 251–254]. Due to the non-collinear magnetic structure that breaks time-reversal symmetry in a non-trivial way seen below  $T_N$  in  $UO_2$ , the existence of piezo-

magnetism is possible[255]. The piezomagnetic effect (together with trigonal distortion upon applied magnetic field along 111 direction) has recently been observed in  $\text{UO}_2$  crystals[249], revealing broken time-reversal symmetry and strong coupling between uranium magnetic moments and lattice degrees of freedom.

### 3. Neptunium Dioxide: $\text{NpO}_2$

$\text{NpO}_2$  crystallizes in the same *fcc* fluorite structure as the other actinide oxides, with a lattice parameter of  $5.434\text{\AA}$ [188]. Based on the ionic picture, the  $5f^3$  configuration for  $\text{Np}^{4+}$  ions in  $\text{NpO}_2$  predicts the crystal field ground state to be a magnetic doublet, suggesting the smallest amount of magnetic exchange could result in subsequent magnetic ordering. Early magnetic susceptibility and specific heat measurements [256] suggested a magnetic phase transition  $T_0$  at 25 K. Although  $\text{NpO}_2$  is isostructural to  $\text{UO}_2$  and the entropy calculated from the specific heat below the phase transition ( $T_0 = 25$  K) is very similar to that of  $\text{UO}_2$ [257], the magnetic ground state of  $\text{NpO}_2$  turned out to be complex [258]. Despite the magnetic phase transition suggested by earlier experiments, low-temperature neutron diffraction[259–261] and Mössbauer[262, 263] experiments have failed to identify an ordered magnetic moment. Fried et al.[263] later revisited the low-temperature Mössbauer measurements down to 1.5 K with an applied magnetic field up to 8 T suggesting no dipole magnetism and that the phase transition  $T_0$  can be attributed to a hypothesized competitive structural transition. However, this structural transition, consisting of a JT distortion of the oxygen cage, has not been experimentally confirmed[258].

To understand the phase transition  $T_0$  of  $\text{NpO}_2$  and address the experimental inconsistencies, Zolnierok et al.[264] hypothesized the cation is trivalent in  $\text{NpO}_2$ . However, crystal field measurements using neutron spectroscopy displayed an inelastic peak originating from excitations between the  $\Gamma_8^2$ , and  $\Gamma_8^1$  crystal field quartets and crystal field parameters are consistent with  $\text{Np}^{4+}$  ions[265]. The observed ordering in  $\text{NpO}_2$  with no net magnetic moment could be explained by quadrupolar ordering[266]. However, this cannot account for the observation of a temperature-independent susceptibility[224] and the asymmetry in the muon experiments[267]. However, octupolar ordering in  $\text{NpO}_2$  could explain the essentially ‘zero’ moment of Mössbauer spectroscopy and the asymmetry in the muon experiments. The possibility of having octupolar magnetic ordering in  $\text{NpO}_2$  has been studied from a theoretical perspective[268, 269]. A resonant X-ray scattering study performed at the Np  $M_{4,5}$  edges below  $T_0$  has shown a growth of superlattice Bragg peaks related to the long-range order of Np electric quadrupoles[266, 270] and a complex ordering of higher-order magnetic multipoles, which lead to a singlet ground state with zero dipole-magnetic moment[1, 6, 271, 272]. Unlike  $\text{UO}_2$ , no sym-

metry change have been observed in  $\text{NpO}_2$ , and recent neutron powder diffraction data collected down to 300 mK showed no significant changes in the diffraction pattern below and above  $T_0 = 25$  K[273]. Frontzek et al.[273] suggested that neutron single crystal diffraction on  $\text{NpO}_2$  could improve the detection limit for octupolar order.

### 4. Plutonium Dioxide: $\text{PuO}_2$

Despite  $\text{PuO}_2$  being used in the nuclear fuel industry and being the subject of nearly 80 years of research, its ground state is still a subject of extensive studies.  $\text{PuO}_2$  also crystallizes in the same *fcc* fluorite structure as the other actinide oxides, with a lattice parameter of  $a = 5.395\text{\AA}$ [188]. Laser heating studies have shown  $\text{PuO}_2$  melts at  $3017(28)$  K[274], several hundred degrees higher than the previously cited melting point of 2700 K[275]. Recent X-ray absorption near edge spectroscopy (XANES) and X-ray absorption fine structure (EXAFS) measurements suggest an optical band gap of  $2.8(1)$  eV at room temperature[275]. Furthermore, the low-temperature electronic contribution to the specific heat in  $\text{PuO}_2$  can be extrapolated to zero at  $T = 0$ , in agreement with its Mott-insulating ground state [41].

Based on the ionic picture, the  $\text{Pu}^{4+}$  ion with a  $5f^4$  configuration in  $\text{PuO}_2$  suggests the crystal field ground state to be a  $\Gamma_1$  singlet[276, 277]. The presence of a non-magnetic ground state in  $\text{PuO}_2$  is supported by the specific heat of  $\text{PuO}_2$  (polycrystalline samples) that shows no anomaly in the  $C_p(T)$ [41]. Early experimental evidence pointed to a paramagnetic ground state with a constant magnetic susceptibility of  $0.54 \times 10^{-3} \text{ cm}^3 \text{ mol}^{-1}$  up to 1000 K [212] suggesting Van Vleck paramagnetism due to the crystal electric field transition between the  $\Gamma_1$  ground state and the  $\Gamma_4$  state [212]. This understanding was confirmed through inelastic neutron scattering (INS) measurements; however, the transition was measured to be  $123 \text{ meV}$ , suggesting a magnetic susceptibility of  $\sim 1 \times 10^{-3} \text{ cm}^3 \text{ mol}^{-1}$ [278]. The constant magnetic susceptibility measured in between 4 – 1000 K [212] estimated the transition energy for  $\Gamma_1 \rightarrow \Gamma_4$  to be  $\approx 284 \text{ meV}$ , much higher than measured from the INS experiments. Subsequent NMR measurements confirmed the absence of any magnetic order or structural distortions down to 6 K, verifying the temperature independence of the magnetic susceptibility[213].

It is worth mentioning that the magnetic ground state of  $\text{PuO}_2$  is a subject of ongoing, mostly theoretical, studies that might suggest the existence of antiferromagnetic order in this system. A first-principles calculation of the crystal field scheme reported the transition energy for  $\Gamma_1 \rightarrow \Gamma_4$  to be  $99 \text{ meV}$ , which is relatively close to the INS value of  $123 \text{ meV}$  and introduced the idea of an antiferromagnetic exchange interaction between the  $\text{Pu}^{4+}$  ions[279]. Recently, Pegg et al.[32, 216] suggested a longitudinal  $3k$  AFM structure that retains the  $Fm\bar{3}m$  symmetry and the calcu-

lated band gap (2.97 eV) associated with this magnetic structure agrees well with experimental optical band gap of 2.8(1) eV at room temperature[275], indicating the need to consider noncollinear and spin-orbit interactions in PuO<sub>2</sub>. Furthermore, the first principles local density +  $U$  (LDA+U) and generalized gradient +  $U$  (GGA+U) approximations have also predicted an AFM ground state for PuO<sub>2</sub>[214, 215].

### 5. Americium Dioxide: AmO<sub>2</sub>

AmO<sub>2</sub> crystallizes in the same *fcc* fluorite structure as the other actinide dioxides, with a lattice parameter of 5.379Å[280]. Although AmO<sub>2</sub> is a simple tetravalent oxide isostructural to UO<sub>2</sub> and NpO<sub>2</sub>, the magnetic ground state of AmO<sub>2</sub> is poorly understood due to the rarity of its parent actinide, along with the more serious limiting factor with experiments, the strong self-radiation-induced crystalline disorder that arises due to the continuous  $\alpha$ -particle decay of Am[14]. Despite these difficulties, more than 40 years ago, a phase transition was observed near  $T_0 = 8.5$  K through magnetic susceptibility experiments demonstrating an effective moment of 1.31  $\mu_B$  and suggesting the ground state of Am<sup>4+</sup> to be a  $\Gamma_7$  doublet carrying a dipole degree of freedom[281, 282]. At the time, a comparison was made with the antiferromagnetic order seen in UO<sub>2</sub>; however, Mössbauer[33] and neutron diffraction measurements failed to detect any AFM order[34]. More recently, the  $\Gamma_7$  doublet has been shown to be converted to a  $\Gamma_8$  quartet through spin-orbit couplings and Coulomb Interactions[283]. Since, the  $\Gamma_8$  quartet can carry not only dipole but also quadrupolar and octupolar moments, it hints at the possibility of multipolar ordering in AmO<sub>2</sub>[283, 284].

The first and subsequent NMR measurements on AmO<sub>2</sub> done by Tokunaga *et al.* confirmed the phase transition seen at  $T_0 = 8.5$  K[14, 15]. The signal wipe-out below 12 K and a broadening of the spectrum with a randomly distributed hyperfine field developing at the lowest temperature of 1.5 K[14] revealed short-range, spin-glass-like character for the magnetic phase transition seen at  $T_0$ . The NMR data was remarkably similar to that of a geometrically frustrated antiferromagnetic NiGa<sub>2</sub>S<sub>4</sub>[285]. Over the course of the experiment, significant NMR intensity change occurred, indicating the electronic ground state is extremely sensitive to disorder induced by self-irradiation through the decay of Am[14]. Moreover, the NMR spectrum of AmO<sub>2</sub> is rather different from that seen in the antiferromagnetic ground state of UO<sub>2</sub> or the multipolar ground state of NpO<sub>2</sub>[211]. The intense radioactivity and self-induced disorder present in any AmO<sub>2</sub> powder sample make experimentation particularly delicate and, thus, limit the available experimental techniques. Hence, detailed characterization on AmO<sub>2</sub> is severely lacking. Single crystal neutron scattering, NMR, Muon spin relaxation ( $\mu$ SR), or even a specific heat study could help reveal the exact nature of the phase transition

observed in AmO<sub>2</sub>.

### 6. Curium Dioxide: CmO<sub>2</sub>

Like PuO<sub>2</sub> and AmO<sub>2</sub>, CmO<sub>2</sub> is lacking in experimental data, and the existing data sometimes contradict one another. CmO<sub>2</sub> crystallizes in the shared *fcc* fluorite structure with a lattice constant of 5.359(2) Å[165]. In theory, the Cm<sup>4+</sup> ion with a  $5f^6$  configuration in CmO<sub>2</sub> should exhibit a singlet ground state with  $J = 0$  and therefore, be nonmagnetic. Yet, magnetic susceptibility measurements of CmO<sub>2</sub> show a Curie-Weiss behavior (instead of temperature independence) and a large effective moment of 3.36(6)  $\mu_B$ [51, 193]. Morss *et al.*[193] determined that no long-range order was present in CmO<sub>2</sub> using neutron diffraction measurements, indicating the absence of any oxygen superlattice or superstructure and carefully determined the sample was stoichiometric CmO<sub>2</sub> without additional phases.

Niikura *et al.*[286] predicted the excitation energy between the ground and magnetic excited states become small due to the combined effect of Coulomb interactions, spin-orbit coupling, and crystal electric field potential and could be responsible for the magnetic behavior of CmO<sub>2</sub>. The lattice parameters of CmO<sub>2</sub> deviate from the actinide contraction (a steady decrease in lattice parameters as the atomic number increases in the Actinide Series), suggesting a possible mixed-valence configuration for Cm atoms in CmO<sub>2</sub>[19, 20]. Recently, Huang *et al.*[20] theorized the Cm ions in CmO<sub>2</sub> consist of such a mixed-valence electronic structure between the  $5f^6$  and  $5f^7$  configurations. The Cm<sup>3+</sup> ion with  $5f^7$  could contribute a moment up to 7.94 $\mu_B$ . In this mixed-valence scenario, the effective magnetic moment agrees well with the experimental value[20]. However, these theoretical models for CmO<sub>2</sub> have not been confirmed by experiments. Making matters worse, CmO<sub>2</sub> does not appear to be an insulator with a large band gap like the other actinide oxides; rather, the band gap is predicted to be small, on the order of  $\sim 0.4$  eV [287, 288]. High-temperature magnetic susceptibility and X-ray absorption spectroscopy experiments may provide further insight into the mixed-valence scenario suggested for CmO<sub>2</sub>.

### 7. Berkelium Dioxide: BkO<sub>2</sub>

Following the discovery of americium and curium, berkelium (Bk) and californium were produced and discovered via nuclear bombardment in 1949-50. However, due to the difficulty in production, the most stable isotope of Berkelium, <sup>247</sup>Bk is not commonly used for experimental work; rather the <sup>249</sup>Bk isotope is the only isotope available in bulk form, and thus is used for experimental studies [4, 289]. BkO<sub>2</sub> also crystallizes in the same *fcc* fluorite structure shared by the other actinide dioxides

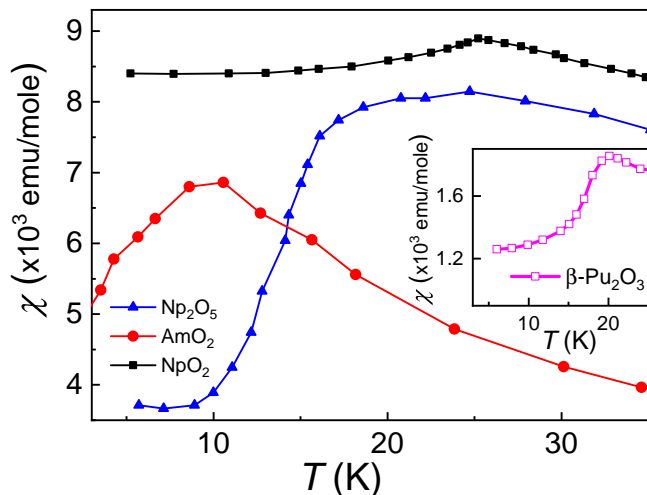


FIG. 2. Magnetic susceptibility of  $\text{NpO}_2$ [224],  $\text{AmO}_2$ [227],  $\beta\text{-Pu}_2\text{O}_3$ [225] and  $\text{Np}_2\text{O}_5$ [141] as a function of temperature showing a cusp anomaly related to magnetic phase transitions.

with a lattice parameter of  $5.334(5)$  Å[168]. In  $\text{BkO}_2$ , berkelium exhibits the same 4+ oxidation state as the other actinide dioxides, therefore exhibiting a half-filled  $5f^7$  electronic configuration with a total angular momentum  $L = 0$ .

Early electron paramagnetic resonance (EPR)[290] and magnetic susceptibility[226] experiments determined the ground state to be the  $\Gamma_6$  doublet, while the  $\Gamma_8$  quartet followed by  $\sim 6 - 10$  meV. These measurements used  $\text{BkO}_2$  in a  $\text{ThO}_2$  matrix. The magnetic susceptibility displayed two temperature-dependent paramagnetic regions with effective moments of  $7.66 \mu_B$  (10 to 95 K) and  $5.8 \mu_B$  (95 to 220 K) while below 10 K, the data suggests a possible AFM transition at 3 K[226]. Later, *Nave et al.*[51] reported an effective moment of  $7.92 \mu_B$  (a localized  $5f^7$  configuration) as found by a Curie-Weiss fit to the magnetic susceptibility (50-300 K) with a large Weiss temperature  $\theta_W = 250(50)$  K. Calculating the crystal field levels using the perturbative model proposed by *Magnani et al.*, finds agreement with the ground state levels. However, the energy splitting is significantly smaller ( $\sim 1$  meV) than experimental estimates (6-10 meV)[226, 290, 291]. Recently, *Putkov et al.*[289] calculated the electronic structure and XPS spectrum for the valence electrons of  $\text{BkO}_2$  in the 0 to 50 eV range, finding excellent agreement with the experimental XPS spectrum[292] and suggesting covalence between orbitals plays a major role in  $\text{BkO}_2$ . Neutron diffraction, NMR or  $\mu\text{SR}$  measurements are critical to resolve the nature of the phase below the  $T = 3$  K magnetic susceptibility phase transition.

## 8. Californium Dioxide: $\text{CfO}_2$

Californium, like berkelium, is one of the last elements to be discovered in the actinide series.  $\text{CfO}_2$  crystallizes in the same *fcc* fluorite structure shared by the other actinide dioxides with a lattice parameter of  $5.310(2)$  Å[169]. Californium can adopt a range of oxidation states ranging from 2+ to 5+[293] and in  $\text{CfO}_2$ , californium exhibits a 4+ oxidation state, yielding a  $5f^8$  electronic configuration and a  $J = 6$  multiplet. Magnetic susceptibility experiments determined that this multiplet is heavily split by crystal electric fields between 20 and 100 K and  $\text{CfO}_2$  exhibited antiferromagnetic ordering below  $T_N = 7$  K[294]. Above 100 K,  $\text{CfO}_2$  displays Curie-Weiss behavior with an effective moment  $\mu_{eff} = 9.1(2) \mu_B$ , in agreement with the theoretical moment of  $9.3 \mu_B$ [294]. *Magnani et al.*[291] proposed a perturbative model for the crystal electric fields in the actinide elements and determined the ground state of  $\text{CfO}_2$  is the  $\Gamma_3$  doublet with one of the  $\Gamma_5$  triplets laying only 3.5 meV higher. The calculated magnetic susceptibility of this perturbative model agrees exceptionally well with existing experimental magnetic susceptibility data[294].

## 9. $\text{PaO}_2$

Protactinium (Pa) has no current uses outside of scientific research, and in combination with its activity, rarity, and toxicity, it is one of the least studied and understood actinide elements. While protactinium can form various compounds with oxidation states ranging from 2+ to 5+, it is most commonly present in the 5+ oxidation state where it forms the pentoxide  $\text{Pa}_2\text{O}_5$ . Reduction of the pentoxide using hydrogen at  $1550$  °C forms the dioxide  $\text{PaO}_2$ , where Protactinium takes a 4+ oxidation state with a  $5f^1$  electronic configuration[74].  $\text{PaO}_2$  crystallizes in the *fcc* structure with a lattice constant of  $5.505(1)$  Å[74]. Recently, *Obodo et al.* predicted  $\text{PaO}_2$  to be a Mott-Hubbard insulator with a band gap of  $3.48$  eV[295]; however, no experimental studies have been made for comparison.

## B. Magnetic properties of sesquioxides

### 1. $\text{Cf}_2\text{O}_3$

In the lanthanide sesquioxides, three crystal structures are known (the  $\text{M}_2\text{O}_3$  structures): the body-centered cubic (*bcc*)  $\text{Mn}_2\text{O}_3$  structure, the hexagonal  $\text{La}_2\text{O}_3$  structure, and the monoclinic  $\text{Sm}_2\text{O}_3$  structure.  $\text{Cf}_2\text{O}_3$  is known to crystallize in the monoclinic  $\text{Sm}_2\text{O}_3$  type (lattice parameters  $a = 14.124(20)$  Å,  $b = 3.591(3)$  Å,  $c = 8.809(13)$  Å)[199], as well as the cubic  $\text{Mn}_2\text{O}_3$  structure (lattice parameter  $a = 10.839(4)$  Å) [170]. Californium exhibits a 3+ oxidation state in the sesquioxide  $\text{Cf}_2\text{O}_3$ , yielding a  $5f^9$  electronic configuration. Both cubic

and monoclinic structures of  $\text{Cf}_2\text{O}_3$  exhibit Curie-Weiss behavior above 100 K with effective moments  $\mu_{eff} = 9.8(2)\mu_B$  (*bcc*) and  $\mu_{eff} = 10.2(2)\mu_B$  (monoclinic)[294]. Moore et al.[294] reported both structures exhibit AFM ordering with  $T_N = 19.0(1.5)$  K for cubic and  $T_N = 8(2)$  K for monoclinic structure, while in between 20 and 100 K, the magnetic susceptibilities displayed pronounced crystal field effects. However, later Morss et al.[170] reported no magnetic ordering down to 1.5 K based on their magnetic susceptibility measurements on *bcc*  $\text{Cf}_2\text{O}_3$ . Morss et al.[170] noted that their study used 1.23 mg sample for magnetic susceptibility measurements, which is significantly larger than the 31  $\mu\text{g}$  sample used by Moore et al.[294] and the magnetic ordering could have been impacted due to significantly more radioactive self-heating. The magnetism of  $\text{Cf}_2\text{O}_3$  is not yet fully resolved and single crystal neutron diffraction, magnetic susceptibility, or  $\mu\text{SR}$  studies could resolve the magnetic ordering observed in  $\text{Cf}_2\text{O}_3$ .

## 2. $\text{Cm}_2\text{O}_3$

$\text{Cm}_2\text{O}_3$  exhibits all three known  $\text{M}_2\text{O}_3$  structure types as well as two additional high-temperature polymorphic phases[296]; above 1615 °C  $\text{Cm}_2\text{O}_3$  forms the hexagonal  $\text{La}_2\text{O}_3$  structure, between 800 – 1615 °C the monoclinic  $\text{Sm}_2\text{O}_3$  structure forms, and below 800 °C, the *bcc*  $\text{Mn}_2\text{O}_3$  structure forms[159, 297]. Lattice parameters for the hexagonal structure are  $a = 3.80(2)\text{Å}$ ,  $c = 6.00(3)\text{Å}$  at 1750 °C, [195, 298], for the monoclinic structure are  $a = 14.282(8)\text{Å}$ ,  $b = 3.652(3)\text{Å}$ ,  $c = 8.900(5)\text{Å}$ ,  $\beta = 100.31(5)^\circ$ [162], and for the *bcc* structure  $a = 10.97(1)\text{Å}$ [195]. In  $\text{Cm}_2\text{O}_3$ , curium exhibits the same 3+ oxidation state as the other sesquioxides, therefore exhibiting a half-filled  $5f^7$  configuration with total angular momentum  $L = 0$ . So,  $\text{Cm}_2\text{O}_3$  could exhibit the  $\Gamma_6$  doublet ground state like in  $\text{BkO}_2$ ; however, this has yet to be verified.

Magnetic susceptibility experiments determined monoclinic  $\text{Cm}_2\text{O}_3$  exhibits Curie-Weiss behavior between 100 – 300 K with  $\mu_{eff} = 7.89(4)\mu_B$  whereas the calculated moment for the free ion is  $7.94\mu_B$ [159]. Furthermore, Morss et al.[159] reported low-temperature antiferromagnetic ordering below 13(2) K[159]. Sample preparation using the very long-lived  $^{248}\text{Cm}$  (half-life =  $3.39 \times 10^5$  year) isotope over the high  $\alpha$  specific activities of the most common  $^{242}\text{Cm}$  (half-life = 163 days) isotope could enable further physical property characterization on this compound beyond the known current crystal structures[159]. Neutron diffraction,  $\mu\text{SR}$ , and specific heat studies are needed to further understand magnetic properties of  $\text{Cm}_2\text{O}_3$ .

## 3. $\text{Am}_2\text{O}_3$

$\text{Am}_2\text{O}_3$ , like its dioxide  $\text{AmO}_2$ , is very poorly understood. Like the other actinide sesquioxides,  $\text{Am}_2\text{O}_3$  is known to crystallize in the three  $\text{M}_2\text{O}_3$  structures: the *bcc*  $\text{Mn}_2\text{O}_3$  structure, the hexagonal  $\text{La}_2\text{O}_3$ , and the monoclinic  $\text{Sm}_2\text{O}_3$  structure. Lattice parameters for the hexagonal structure are  $a = 3.8123(3)\text{Å}$ ,  $c = 5.9845(5)\text{Å}$ [155, 191, 192], for the monoclinic structure are  $a = 14.315(2)\text{Å}$ ,  $b = 3.6793(5)\text{Å}$ ,  $c = 8.927(1)\text{Å}$ ,  $\beta = 100.37(2)^\circ$  [191, 192], and for the *bcc* structure  $a = 11.012(5)\text{Å}$ [155, 192]. The monoclinic  $\text{Am}_2\text{O}_3$  is reported to have O/Am ratios between 1.54 and 1.51[192] and has never been isolated alone[299].

XAFS measurements[300] show excellent agreement with existing X-ray diffraction data and theoretical predictions using the Full-Potential Linearized Augmented Plane Wave (FP-LAPW) method in DFT, indicating the electronic structure and formation enthalpies of hexagonal  $\text{Am}_2\text{O}_3$  can be modeled successfully using DFT[155, 299–301]. Recently, modeling using the GGA+U as well as hybrid functionals has predicted hexagonal  $\text{Am}_2\text{O}_3$  to be a Mott insulator with a band gap around 2.85 eV ( $U = 5$  eV) and determined it is the most stable form at low temperatures[299, 302]. Unlike  $\text{AmO}_2$ , americium in  $\text{Am}_2\text{O}_3$  exhibits a 3+ oxidation state in the sesquioxide, yielding a  $5f^6$  electronic configuration with  $J = 0$ . Thus,  $\text{Am}_2\text{O}_3$  may have a non-magnetic ground state yet to be experimentally verified.

## 4. $\text{Pu}_2\text{O}_3$

$\beta\text{-Pu}_2\text{O}_3$  crystallizes in the hexagonal  $\text{La}_2\text{O}_3$  structure shared with the other actinide sesquioxides as well as  $\text{Nd}_2\text{O}_3$ [303, 304], with lattice parameters  $a = 3.841(6)\text{Å}$  and  $c = 5.958(5)\text{Å}$ [189]. In  $\text{Pu}_2\text{O}_3$ , plutonium exhibits a 3+ oxidation state, yielding a  $5f^5$  electronic configuration with a Kramer's doublet ground state. A heat capacity anomaly associated with an antiferromagnetic transition  $T_N = 19$  K[225] was measured by Flotow et al.[142]. Mccart et al.[225] reported two magnetic transitions ( $T_N = 19$  K and  $T = 4$  K) in  $\beta\text{-Pu}_2\text{O}_3$  from neutron diffraction and magnetic susceptibility measurements. Later Wulff et al.[305] solved the magnetic structures below both magnetic transitions by performing neutron powder diffraction. The magnetic structure below  $T_N = 19$  K was described by a magnetic cell that is doubled relative to the chemical unit cell in all three crystallographic directions and below 4 K the magnetic cell is identical to the chemical unit cell. The magnetic moment was found to be  $0.60(2)\mu_B$  per Pu ion pointing along the unique  $c$  axis at all temperatures below  $T_N$ [305] and is consistent with a Kramer's doublet ground state.

In addition to the stoichiometric  $\beta\text{-Pu}_2\text{O}_3$ , two forms of sub-stoichiometric  $\alpha\text{-Pu}_2\text{O}_3$  sesquioxides are known to exist due to loss of oxygen from the dioxide. The first form,  $\alpha\text{-Pu}_2\text{O}_3$ , has an O/Pu ratio of 1.515 with a *bcc*

structure with lattice parameter  $a = 11.04(2)\text{\AA}$ . The second form,  $\alpha'$ -Pu<sub>2</sub>O<sub>3</sub>, has an O/Pu ratio of 1.61 with a *fcc* structure with lattice parameter  $a = 5.409(1)\text{\AA}$ [189]. A theoretical DFT + *U* study predicts an AFM semiconducting ground state for  $\alpha$ -Pu<sub>2</sub>O<sub>3</sub> with an electronic band gap of 1.40 eV[306], which has yet to be experimentally measured.

### C. Magnetic properties of other actinide oxides

#### 1. U<sub>2</sub>O<sub>5</sub>

U<sub>2</sub>O<sub>5</sub> lies on the transition point between the fluorite structure and the layered structures found in other uranium oxides and is one of the least understood of the various uranium oxides, owing to its instability relative to the other oxides[307]. U<sub>2</sub>O<sub>5</sub> is known to crystallize in at least 4 structures,  $\alpha$ -,  $\beta$ -,  $\gamma$ -, and  $\delta$ -, indicating complicated structures of U<sub>2</sub>O<sub>5</sub>[105, 208]. The crystal symmetry of  $\alpha$ -U<sub>2</sub>O<sub>5</sub> is unknown (Unk.), while  $\beta$ -U<sub>2</sub>O<sub>5</sub> is hexagonal with lattice parameters  $a = b = 3.813\text{\AA}$ ,  $c = 13.180\text{\AA}$ , and the  $\gamma$ -U<sub>2</sub>O<sub>5</sub> is monoclinic with  $a = 5.410\text{\AA}$ ,  $b = 5.481\text{\AA}$ ,  $c = 5.410\text{\AA}$ ,  $\beta = 90.49^\circ$  [105].  $\delta$ -U<sub>2</sub>O<sub>5</sub> crystallizes in the orthorhombic structure (*Pnma* space group) with  $a = 6.849\text{\AA}$ ,  $b = 8.274\text{\AA}$ , and  $c = 31.706\text{\AA}$ [208] and contains a mixture of distorted O coordination geometries (6- and 7-fold).

Recently,  $\delta$ -U<sub>2</sub>O<sub>5</sub> was successfully modeled using the DFT+*U* method suggesting only U<sup>5+</sup> to be present[308]. All U<sub>2</sub>O<sub>5</sub> structures,  $\alpha$ -,  $\beta$ -,  $\gamma$ -, and  $\delta$ -, are predicted to be insulators with band gaps of 2.01, 2.23, 2.19, and 1.60 eV, respectively[308]. DFT has also shown  $\delta$ -U<sub>2</sub>O<sub>5</sub> to have the highest formation energy of any known uranium oxide [309]. Using the GGA+*U* method in DFT predicted that Np<sub>2</sub>O<sub>5</sub> structured U<sub>2</sub>O<sub>5</sub> is just slightly more stable than  $\delta$ -U<sub>2</sub>O<sub>5</sub> under ambient conditions and no thermodynamic studies have been reported for it, suggesting a new avenue of work in low-temperature uranium oxides[307].

#### 2. Np<sub>2</sub>O<sub>5</sub>

NpO<sub>2</sub> and Np<sub>2</sub>O<sub>5</sub> are the only two stable oxides of neptunium. NpO<sub>2</sub> has been extensively studied from both experimental and theoretical studies compared to Np<sub>2</sub>O<sub>5</sub> and studies on Np<sub>2</sub>O<sub>5</sub> are severely lacking[141, 310, 311]. Forbes et al.[141] reported the structure of Np<sub>2</sub>O<sub>5</sub> to be monoclinic (*P2/c* Space Group) with lattice parameters  $a = 8.168(2)\text{\AA}$ ,  $b = 6.584(1)\text{\AA}$ ,  $c = 9.313(1)\text{\AA}$  and  $\beta = 116.09(1)^\circ$  and to contain three symmetrically distinct neptunyl(V) ions.

In Np<sub>2</sub>O<sub>5</sub>, neptunium exhibits a 5+ oxidation state, yielding a  $5f^2$  electronic configuration. Magnetic susceptibility data on a polycrystalline sample revealed a cusp at 22(3) K, suggesting long-range antiferromagnetic ordering. An effective moment of 2.2(1)  $\mu_B$  and a Weiss constant of  $-43(5)$  K were extracted from the

Curie-Weiss fit[141]. The effective moment is significantly smaller than the free ion value of 3.58  $\mu_B$  and may result from crystal-field effects on the *f*-spin states. Np<sub>2</sub>O<sub>5</sub> could exhibit complex magnetic structures due to the three distinct Np crystallographic sites and the Np-O-Np superexchange pathways, which are impacted by bond lengths and angles. Yun et al.[310] predicted Np<sub>2</sub>O<sub>5</sub> to have insulating behavior and complicated noncollinear magnetic order with a ferromagnetic (FM) exchange coupling along the *c* axis and a weaker antiferromagnetic coupling in the *a* – *b* plane. Experiments like neutron diffraction and magnetic susceptibility on Np<sub>2</sub>O<sub>5</sub> single crystals are essential to understand the exact magnetic ground state and examine the impact of multiple Np sites and the Np-O-Np superexchange pathway in generating competing exchange interactions leading to long-range magnetic order.

#### 3. Pa<sub>2</sub>O<sub>5</sub>

Despite Pa<sub>2</sub>O<sub>5</sub> being the most stable protactinium oxide, the ground state and crystal structure are still poorly understood. The only experimental study on Pa<sub>2</sub>O<sub>5</sub> was undertaken by *Sellers et al.* in 1954, and reported not only an *fcc* structure with a lattice constant of 5.455(7)  $\text{\AA}$  but a second, layered orthorhombic structure, isostructural with Nb<sub>2</sub>O<sub>5</sub> and Ta<sub>2</sub>O<sub>5</sub> pentoxides[74]. In this orthorhombic structure, the unit cell was found to be 6.92(2) $\text{\AA}$  by 4.02(1) $\text{\AA}$  by 4.18(2) $\text{\AA}$ [74]. In its cubic form, Pa<sub>2</sub>O<sub>5</sub> follows the fluorite cubic structure with the additional oxygen atoms randomly occupying available holes [74]. Recently, *Liu et al.*[312] has shown that doping excess oxygen atoms into the octahedral position of Protactinium is the most stable doping position for the fluorite structure and even predicted Pa<sub>2</sub>O<sub>5</sub> to crystallize in the  $\zeta$ -Nd<sub>2</sub>O<sub>5</sub> structure, resulting in a charge-transfer insulator with a band gap of 2.67 eV. This  $\zeta$ -Pa<sub>2</sub>O<sub>5</sub> phase has not been experimentally observed; however due to the aforementioned lack of protactinium oxide investigations it remains a possibility. Recent work on the excitation spectrum of protactinium has shown significant underestimations of the density of states, which needs to be considered in any future theoretical work on the protactinium oxides[313]. The synthesis of single crystals of Pa<sub>2</sub>O<sub>5</sub> and performing single crystal X-ray diffraction (XRD) are key to resolving the existing ambiguity in the exact crystal structure. Furthermore, the availability of high-quality crystals will provide an opportunity to probe the thermodynamic properties of Pa<sub>2</sub>O<sub>5</sub>.

#### 4. U<sub>3</sub>O<sub>8</sub>

Triuranium octoxide, U<sub>3</sub>O<sub>8</sub>, can be formed through oxidation of UO<sub>2</sub> and is one of the most stable forms of uranium under environmental conditions. U<sub>3</sub>O<sub>8</sub> is reported to crystallize in two common polymorphs ( $\alpha$ -

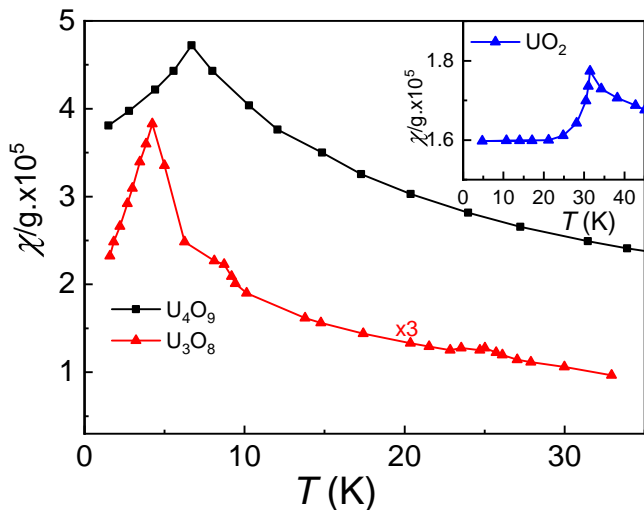


FIG. 3. Magnetic susceptibility per g of  $\text{UO}_2$  (in inset)[221],  $\text{U}_3\text{O}_8$ [221] and  $\text{U}_4\text{O}_9$ [221] as a function of temperature showing a cusp anomaly related to a magnetic phase transition. Note: Magnetic susceptibility of  $\text{U}_3\text{O}_8$  is multiplied by 3 times the original susceptibility values for the better visibility of the phase transitions within the frame.

$\text{U}_3\text{O}_8$  and  $\beta\text{-U}_3\text{O}_8$ ). At room temperature,  $\alpha\text{-U}_3\text{O}_8$  crystallizes in an orthorhombic  $Amm2$  structure while upon heating  $\alpha\text{-U}_3\text{O}_8$  to 1350 °C, an expansion along the  $c$ -direction along with an accompanying contraction along the  $b$ -direction induces an isomorphous transition in structure to the  $P62m$  phase at 573 K[110, 314, 315]. The low temperature  $Amm2$   $\alpha\text{-U}_3\text{O}_8$  phase has two distinct crystallographic sites, one U(VI) site and one double degenerate U(V) site ( $2\text{U(V)}$ ), while the high temperature  $P62m$   $\beta\text{-U}_3\text{O}_8$  phase has only a single crystallographic site[206, 308, 310, 316].  $\alpha\text{-U}_3\text{O}_8$  is semiconducting with a band gap of  $\approx 1.80$  eV[206].

Early magnetic susceptibility experiments displayed three distinct peaks, a single large peak at 4.2 K, and two other small peaks at 8 and 25.3 K, as shown in Fig. 3 [221]. Heat capacity measurements also displayed a peak at 25.3 K[222]. Recent INS experiments confirmed AFM below 22 K (onset between 25 and 22 K) down to at least 1.7 K, with peaks corresponding to  $[0.5\ 1\ 1]$  and  $[0.5\ 2\ 2]$  in an orthorhombic structure[316]. No magnetic intensity was observed at  $[0.5\ 1\ 1]$ , ruling out AFM order along the  $a$  axis[316, 317]. A quasielastic scattering term appears above 100 K, increasing in intensity and width up to 600 K, confirming  $\alpha\text{-U}_3\text{O}_8$  is a mixed-valence state system, similar to  $\text{CmO}_2$ [316]. *Isbill et al.*[312] recently used DFT to show that antiferromagnetic ordering along the  $[0.5\ 1\ 1]$  is indeed lower in energy than along any Miller indices. *Isbill et al.*[312] determined that moments which point along the in-plane directions will gradually relax until they point along a direction between the two distinct crystallographic uranium sites in rather complex noncollinear structures.

## 5. $\text{U}_4\text{O}_9$

$\text{U}_4\text{O}_9$  is formed in the process of oxidizing  $\text{UO}_2$  to  $\text{U}_3\text{O}_8$  and crystallizes in three structures ( $\alpha$ -,  $\beta$ -, and  $\gamma$ -) which are based on the fluorite crystal structure of  $\text{UO}_2$ .  $\alpha$ - and  $\beta\text{-U}_4\text{O}_9$  form similar super-structures to that of  $\text{UO}_2$ , but with a unit cell 4 times larger. In cubic  $\beta\text{-U}_4\text{O}_9$ , additional oxygen atoms are “accommodated” in cuboctahedral clusters (space group  $I43d$ ) whose centers are unoccupied[101, 318, 319]. In  $\alpha\text{-U}_4\text{O}_9$  the same cuboctahedral clusters form, however, the positions are slightly displaced due to a shift in the position of the central atom (trigonal distortion) and are extremely similar to that of  $\text{U}_3\text{O}_8$ [209]. These clusters form layered sheets which transform driven by shear transformations from  $\alpha\text{-U}_4\text{O}_9$  into  $\text{U}_3\text{O}_8$  sheets[21, 209] and this transformation has been shown to be accompanied by a complex change in U oxidation states[320]. Raman spectroscopy has recently determined a band at  $630\text{ cm}^{-1}$  in  $\text{U}_4\text{O}_9$  determined to be characteristic of clusters composed of the excess “accommodated” interstitial oxygen atoms[321]. Neutron diffraction measurements have shown  $\beta\text{-U}_4\text{O}_9$  to be crystallographically ordered with no Uranium-Oxygen bonds shorter than 2.2 Å while  $\alpha\text{-U}_4\text{O}_9$  was shown to have some Uranium-Oxygen bonds on the order of 1.8 Å[209, 322].

Recent high energy resolution limited fluorescence detection X-ray absorption near edge spectroscopy (HERFD-XANES) measurements[323] have shown uranium adopts a mixed valence configuration in  $\text{U}_4\text{O}_9$ , with  $\text{U}^{4+}$  and  $\text{U}^{5+}$  oxidation states[21]. The high temperature ( $T = 77$  to 500 K) magnetic susceptibility experiments determined paramagnetic behavior in  $\text{U}_4\text{O}_9$ [223]. The low-temperature ( $T = 1.5$  to 44 K) magnetic susceptibility measurements reported a maximum at 6.4 K[221]. However, the low-temperature phase transition at 6.4 K was not observed in specific heat measurements[95, 324]. New magnetic susceptibility and specific heat measurements with improved experimental techniques and improved synthesis routes could resolve ambiguity around the low-temperature phase transition observed at 6.4 K.

## 6. $\text{U}_3\text{O}_7$

$\text{U}_3\text{O}_7$  is another oxide formed during the oxidation of  $\text{UO}_2$  to  $\text{U}_3\text{O}_8$ . Historically,  $\text{U}_3\text{O}_7$  was thought to crystallize in two structures,  $\alpha$ - and  $\beta\text{-U}_3\text{O}_7$ . However, early experiments failed to differentiate  $\alpha\text{-U}_3\text{O}_7$  from cubic  $\beta\text{-U}_4\text{O}_9$  in the sample[100, 102, 207, 325]. Neutron diffraction studies and DFT have confirmed  $\text{U}_3\text{O}_7$  crystallizes in a fluorite-type structure consisting of cuboctahedral oxygen clusters very similar to  $\text{U}_4\text{O}_9$ [209, 319]; however, the clusters are tilted and skewed from those seen in  $\text{U}_4\text{O}_9$ [98, 207, 309, 326]. The fluorite-like structure can be characterized by a unit cell containing 15 fluorite-like subshells with lattice parameters  $a = b = 5.3900(2)$  Å, and  $c = 5.5490(2)$  Å ( $c/a =$

1.031)[207]. Recent total reflection X-ray fluorescence-based XANES (TXRF-XANES) has shown  $\text{U}_3\text{O}_7$  is a mixed-valence compound, consisting of uranium in both  $\text{U}^{4+}$  and  $\text{U}^{5+}$  states[327]. First principle calculations using the Vienna ab initio simulation (VASP with the projector-augmented wave (PAW) method) and DFT combined with *Perdew, Burke, and Ernzerhof* functionals (PBE+U) to account for exchange-correlation interactions, including spin-orbit coupling, predicts  $\text{U}_3\text{O}_7$  to be a charge-transfer insulator with a band gap of 0.32 eV[328]. Additionally, in such a structure with cuboctahedral clusters,  $\text{U}^{4+}$  and  $\text{U}^{5+}$  are predicted to carry noncollinear magnetic moments of 1.6 and  $0.8\mu_B$  respectively, resulting in the fluorite-based structure having canted FM order in characteristic layers[328]. However, this FM order has yet to be experimentally observed.

### 7. $\text{UO}_3$

Heating uranyl nitrate to 400 °C forms Uranium trioxide,  $\text{UO}_3$ [120], in which uranium takes a 6+ oxidation state. The uranium atoms within  $\text{UO}_3$  can be coordinated with either 6, 7, or 8 oxygen atoms leading to at least 7 known structures,  $\alpha$ -,  $\beta$ -,  $\gamma$ -,  $\delta$ -,  $\varepsilon$ -,  $\zeta$ -, and  $\eta$ - as well as an amorphous  $\text{UO}_3$ [105, 116, 117, 121, 126, 202, 204, 205, 329, 330].  $\alpha$ - $\text{UO}_3$  crystallizes in an orthorhombic structure ( $C2mm$ [202] or  $C222$ [117] space group), while  $\beta$ - $\text{UO}_3$  crystallizes in a monoclinic structure[121] with lattice parameters  $a = 10.34\text{\AA}$ ,  $b = 14.33\text{\AA}$ ,  $c = 3.910\text{\AA}$ , and  $\beta = 99.03^\circ$ [121, 203].  $\gamma$ - $\text{UO}_3$  crystallizes in an orthorhombic structure ( $Fddd$  space group) at room temperature and lower the symmetry to a tetragonal ( $I4_1$  space group) structure at high temperatures[204].  $\delta$ - $\text{UO}_3$  crystallizes in the  $\text{ReO}_3$  structure ( $Pm3m$  space group)[126].  $\varepsilon$ - $\text{UO}_3$  crystallizes in a triclinic ( $P-1$ ) structure with lattice parameters  $a = 4.01\text{\AA}$ ,  $b = 3.85\text{\AA}$ ,  $c = 4.18\text{\AA}$ ,  $\alpha = 98.26^\circ$ ,  $\beta = 90.41^\circ$ , and  $\gamma = 120.46^\circ$ , best described by a  $2\times 1\times 2$  supercell of  $P-1$  with lattice parameters  $a = 8.03\text{\AA}$ ,  $b = 3.86\text{\AA}$ ,  $c = 8.37\text{\AA}$ , and  $\beta = 90.41^\circ$ [128]. Heat capacity and susceptibility measurements on high purity  $\beta$ - and  $\gamma$ - $\text{UO}_3$  suggest weak paramagnetism; however no anomalies were found between 1.3 – 5 K[330]. A recent DFT+U study has predicted three new structures for  $\text{UO}_3$  under 13, 62, and 220 GPa of pressure, predicting a semiconducting phase that transforms under further pressure to semi-metal and metallic phases[331]. DFT+U has predicted a band gap around 1.6 – 2.6 eV for  $\alpha$ - $\text{UO}_3$ , while  $\beta$ -,  $\gamma$ -, and  $\delta$ - $\text{UO}_3$  all have predicted band gaps of  $\sim 2 - 2.4$ ,  $\sim 2.4 - 2.8$ , and  $\sim 2.1 - 2.2$  eV respectively[331–334]. Epitaxial film growths of  $\alpha$ - $\text{UO}_3$  allowed an indirect measurement of the band gap of 2.26 eV[203].

## V. SUMMARY AND OUTLOOK

The present article focuses on synthesis methods and bulk magnetic properties of the known actinide oxides, binaries in particular. We have also included a discussion of their crystal structures and appropriate methods for crystal growth. Since these actinide oxides are insulators and crystallize in relatively simple crystal structures, it might be expected that these compounds and their magnetic behavior would be well understood, both theoretically and experimentally. Contrary to this expectation, however, the magnetic ground states of actinide oxides, other than maybe  $\text{ThO}_2$  and  $\text{UO}_2$ , are still unresolved due to the lack of high-quality samples, especially single crystals, the dual nature of  $5f$  electrons, and the electronic correlations and strong spin-orbit coupling associated with these actinide materials.

An improved understanding of the chemical and physical properties of these actinide materials at low temperature may prompt new areas of actinide research, opening critical avenues for the design and control of novel phenomena related to  $5f$  electrons, including electronic correlations and topology. Moreover, this improved foundational understanding will impact advanced modeling and materials design for high-temperature environments for nuclear industry applications[18, 32]. As detailed in our discussion on crystal growth, a lack of effort and progress in the growth of actinide oxide single crystals hinders the study of their fundamental structural and electronic properties, which are necessary for enabling the above opportunities. For example,  $\text{U}_3\text{O}_8$  forms through further oxidation of  $\text{UO}_2$ , and studying the physical and chemical properties of high-quality crystals of  $\text{U}_3\text{O}_8$  will allow us to gain new knowledge concerning its magnetic ground state, permitting us to develop models for interpreting and explaining uranium chemistry at a fundamental level, and ultimately, enable us to apply such an improved understanding to uranium science and research in the nuclear fuel industry. Therefore, the pursuit of high-quality samples is imperative for unraveling the intricate interplay of factors, including crystal field and strong spin-orbit coupling, which underlie the captivating magnetic behaviors observed in actinide oxides such as  $\text{UO}_2$ ,  $\text{CfO}_2$ ,  $\text{CmO}_2$ ,  $\text{Am}_2\text{O}_3$ , and  $\text{U}_3\text{O}_8$ . Combining efforts of high-quality samples, detailed crystal structures, and magnetic characterization techniques holds the key to unraveling the complexities of magnetic ordering in these materials.

In general, the magnetic properties of the actinide dioxides appear to lack notable trends, however both theoretical models and existing experimental data hint at the possibility of similar ground states common to the various dioxides. For instance, experimental evidence from magnetic susceptibility and X-ray resonant scattering for  $\text{NpO}_2$  suggests a magnetic phase transition at  $T_0 = 25$  K, yet magnetic order has not been observed in neutron diffraction studies. Magnetic susceptibility measurements suggest a phase transition at  $T_0 = 8.5$  K

in AmO<sub>2</sub>, and confirmed through NMR measurements, which suggest short range, glass-like character. However, the possibility of multipolar ordering has not yet been ruled out for AmO<sub>2</sub>, as well as for NpO<sub>2</sub>. UO<sub>2</sub> displays a first order antiferromagnetic transition at  $T_N = 30.8$  K with a  $3 - k$  noncollinear magnetic structure below  $T_N$ . Ultimately, UO<sub>2</sub>, NpO<sub>2</sub>, and AmO<sub>2</sub> might all be reasonably well described by various complicated magnetic structures or multipolar ordering. BkO<sub>2</sub> was suggested to exhibit an AFM transition at  $T = 3$  K, while an AFM transition at  $T_N = 7$  K in CfO<sub>2</sub> was confirmed. In theory, CmO<sub>2</sub> should be nonmagnetic; however, it also displays a temperature-dependent magnetic susceptibility, hinting at the possibility of a multivalent configuration present in this material. Despite the expected ground state for CmO<sub>2</sub> that should be nonmagnetic, it follows the trend set by the heavier BkO<sub>2</sub> and CfO<sub>2</sub>, which both display Curie-Weiss behavior above 100 K. However, whereas below 100 K the magnetic susceptibilities of BkO<sub>2</sub> and CfO<sub>2</sub> become dominated by crystal field effects and subsequent AFM ordering, in CmO<sub>2</sub>, the possibility of a multivalent configuration may complicate the crystal field effects and any subsequent order.

The actinide sesquioxides and higher oxides have been largely understudied and the available data to date is too inconclusive to grasp at potential connections. Cf<sub>2</sub>O<sub>3</sub> follows the trend set by its dioxide, exhibiting Curie-Weiss behavior above 100 K with a large effective moment, and AFM ordering seen at  $T_N = 19(1.5)$  K in the *bcc* structure. That was later revisited with a larger sample suggesting no AFM order, together with  $T_N = 8(2)$  K in the monoclinic structure. Cm<sub>2</sub>O<sub>3</sub> again, follows the same trend, with an AFM transition at  $T_N = 13(2)$  K. Am<sub>2</sub>O<sub>3</sub> may be nonmagnetic; however no experimental measurements have been completed. Pu<sub>2</sub>O<sub>3</sub> exhibits an AFM transition at  $T_N = 19$  K, where the magnetic unit cell is double the chemical unit cell, and a second transition at  $T = 4$  K, where the magnetic unit cell is equal to the chemical unit cell. Magnetic susceptibilities have never been measured for U<sub>2</sub>O<sub>5</sub> and Pa<sub>2</sub>O<sub>5</sub>; however measurements for Np<sub>2</sub>O<sub>5</sub> reveal an AFM transition at 22(3) K that might be explained by a complicated noncollinear magnetic structure which has yet to be verified experimentally. The higher uranium oxides, U<sub>3</sub>O<sub>8</sub> and U<sub>4</sub>O<sub>9</sub> display paramagnetic Curie-Weiss behavior at high temperatures and undetermined phase transitions at 4, 8, and 25.3 K in U<sub>3</sub>O<sub>8</sub> and 6.4 K in U<sub>4</sub>O<sub>9</sub>, respectively. UO<sub>3</sub> displays weak paramagnetic behavior, while U<sub>3</sub>O<sub>7</sub> has

never undergone experimental magnetic characterization, although theory suggests noncollinear magnetic moments resulting in an unverified canted FM order.

At present, despite large previous experimental and theoretical efforts, a vast bounty of scientific knowledge regarding the actinide elements remains untapped, their applications and our understanding constrained by a dearth of needed synthetic and experimental work. It is our hope that this article will serve to alleviate at least some of the factors currently impeding such work, by promulgating further the requisite methods for single crystal syntheses and more broadly advertising the value of those syntheses. High-quality single crystals are critical for the determination of accurate crystal structures and investigations of complex magnetism and relevant electronic and thermodynamic properties, both in the chronically underexplored actinide oxides, as well as in actinide species more broadly. The understanding thus gained will play an indispensable role in unlocking new areas of actinide research (both applied and fundamental), and revealing the full breadth of possibilities the actinides present.

## VI. ACKNOWLEDGMENTS

We thank Garret Gotthelf and Joseph Paddison for useful discussions and comments. B. K. R., A. B., and R. G. acknowledge support from the Laboratory Directed Research and Development (LDRD) program within the Savannah River National Laboratory (SRNL). This work was produced by Battelle Savannah River Alliance, LLC under Contract No. 89303321CEM000080 with the U.S. Department of Energy. Publisher acknowledges the U.S. Government license to provide public access under the DOE Public Access Plan (<http://energy.gov/downloads/doe-public-access-plan>). K.G. acknowledges support from the Division of Materials Science and Engineering, Basic Energy Sciences, Office of Science of the U.S. Department of Energy (U.S. DOE). GM and HzL acknowledge support by the Center for Hierarchical Waste Form Materials (CHWM), an Energy Frontier Research Center (EFRC), supported by the U.S. Department of Energy, Office of Basic Energy Sciences, Division of Materials Sciences and Engineering under Award DE-SC0016574.

- 
- [1] Paolo Santini, Stefano Carretta, Giuseppe Amoretti, Roberto Caciuffo, Nicola Magnani, and Gerard H Lander. Multipolar interactions in f-electron systems: The paradigm of actinide dioxides. *Reviews of Modern Physics*, 81(2):807, 2009.
- [2] Kevin T Moore and Gerrit van der Laan. Nature of the  $5f$  states in actinide metals. *Reviews of Modern Physics*, 81(1):235, 2009.
- [3] ML Marsh and TE Albrecht-Schmitt. Directed evolution of the periodic table: probing the electronic structure of late actinides. *Dalton Transactions*, 46(29):9316–9333, 2017.
- [4] Frankie D White, David Dan, and Thomas E Albrecht-Schmitt. Contemporary chemistry of berke-

- lium and californium. *Chemistry—A European Journal*, 25(44):10251–10261, 2019.
- [5] G Zwicknagl and P Fulde. The dual nature of  $5f$  electrons and the origin of heavy fermions in  $u$  compounds. *Journal of Physics: Condensed Matter*, 15(28):S1911, 2003.
- [6] Y Tokunaga, D Aoki, Y Homma, S Kambe, H Sakai, S Ikeda, T Fujimoto, RE Walstedt, H Yasuoka, E Yamamoto, et al. NMR evidence for higher-order multipole order parameters in  $\text{NpO}_2$ . *Physical review letters*, 97(25):257601, 2006.
- [7] H-H Kung, RE Baumbach, ED Bauer, VK Thorsmølle, W-L Zhang, K Haule, JA Mydosh, and G Blumberg. Chirality density wave of the “hidden order” phase in  $\text{URu}_2\text{Si}_2$ . *Science*, 347(6228):1339–1342, 2015.
- [8] S Carretta, P Santini, R Caciuffo, and G Amoretti. Quadrupolar waves in uranium dioxide. *Physical review letters*, 105(16):167201, 2010.
- [9] R Caciuffo, P Santini, S Carretta, G Amoretti, A Hiess, N Magnani, L-P Regnault, and GH Lander. Multipolar, magnetic, and vibrational lattice dynamics in the low-temperature phase of uranium dioxide. *Physical Review B*, 84(10):104409, 2011.
- [10] SJ Allen Jr. Spin-lattice interaction in  $\text{UO}_2$ . I. ground-state and spin-wave excitations. *Physical Review*, 166(2):530, 1968.
- [11] SJ Allen. Spin-lattice interaction in  $\text{UO}_2$ . II. theory of the first-order phase transition. *Physical Review*, 167(2):492, 1968.
- [12] J Faber Jr, GH Lander, and BR Cooper. Neutron-diffraction study of  $\text{UO}_2$ : Observation of an internal distortion. *Physical Review Letters*, 35(26):1770, 1975.
- [13] J Faber Jr and GH Lander. Neutron diffraction study of  $\text{UO}_2$ : Antiferromagnetic state. *Physical Review B*, 14(3):1151, 1976.
- [14] Yo Tokunaga, Tsuyoshi Nishi, Masami Nakada, Akinori Itoh, Hironori Sakai, Shinsaku Kambe, Yoshiya Homma, Fuminori Honda, Dai Aoki, and Russell E Walstedt. Self-radiation effects and glassy nature of magnetic transition in  $\text{AmO}_2$  revealed by  $\text{O}^{17}$ -NMR. *Physical Review B*, 89(21):214416, 2014.
- [15] Yo Tokunaga, Tsuyoshi Nishi, Shinsaku Kambe, Masami Nakada, Akinori Itoh, Yoshiya Homma, Hironori Sakai, and Hiroyuki Chudo. NMR evidence for the 8.5 K phase transition in americium dioxide. *Journal of the Physical Society of Japan*, 79(5):053705, 2010.
- [16] Yu Prots, M Krnel, M Schmidt, Yu Grin, and E Svanidze. Uranium-mercury complex antiferromagnet:  $\text{UHg}_6$ . *Physical Review B*, 106(6):L060412, 2022.
- [17] Vsevolod Ivanov, Xiangang Wan, and Sergey Y Savrasov. Topological insulator-to-weyl semimetal transition in strongly correlated actinide system  $\text{UNiSn}$ . *Physical Review X*, 9(4):041055, 2019.
- [18] Xiao Zhang, Haijun Zhang, Jing Wang, Claudia Felser, and Shou-Cheng Zhang. Actinide topological insulator materials with strong interaction. *Science*, 335(6075):1464–1466, 2012.
- [19] Lester R Morss, Norman M Edelstein, Jean Fuger, Joseph J Katz, and LR Morss. *The chemistry of the actinide and transactinide elements*, volume 1. Springer, 2006.
- [20] Li Huang, Ruofan Chen, and Haiyan Lu. Reexamining the ground state and magnetic properties of curium dioxide. *Physical Review B*, 102(8):085127, 2020.
- [21] L. Desgranges, G. Baldinozzi, D. Simeone, and H. E. Fischer. Structural Changes in the Local Environment of Uranium Atoms in the Three Phases of  $\text{U}_4\text{O}_9$ . *Inorganic Chemistry*, 55(15):7485–7491, aug 2016.
- [22] Eric J Schelter, Ruilian Wu, Brian L Scott, Joe D Thompson, David E Morris, and Jaqueline L Kiplinger. Mixed valency in a uranium multimetallic complex. *Angewandte Chemie International Edition*, 47(16):2993–2996, 2008.
- [23] Kristen A Pace, Vladislav V Klepov, Anna A Berseneva, and Hans-Conrad Zur Loye. Covalency in actinide compounds. *Chemistry—A European Journal*, 27(19):5835–5841, 2021.
- [24] Alyssa N Gaiser, Cristian Celis-Barros, Frankie D White, Maria J Beltran-Leiva, Joseph M Sperling, Sahan R Salpage, Todd N Poe, Daniela Gomez Martinez, Tian Jian, Nikki J Wolford, et al. Creation of an unexpected plane of enhanced covalency in cerium (III) and berkelium (III) terpyridyl complexes. *Nature communications*, 12(1):7230, 2021.
- [25] Samantha K Cary, Monica Vasiliu, Ryan E Baumbach, Jared T Stritzinger, Thomas D Green, Kariem Diefenbach, Justin N Cross, Kenneth L Knappenberger, Guokui Liu, Mark A Silver, et al. Emergence of californium as the second transitional element in the actinide series. *Nature Communications*, 6(1):6827, 2015.
- [26] Steven D Conradson, Tomasz Durakiewicz, Francisco J Espinosa-Faller, Yong Q An, David A Andersson, Alan R Bishop, Kevin S Boland, Joseph A Bradley, Darrin D Byler, David L Clark, et al. Possible bose-condensate behavior in a quantum phase originating in a collective excitation in the chemically and optically doped mott-hubbard system  $\text{UO}_{2+x}$ . *Physical Review B*, 88(11):115135, 2013.
- [27] Takashi Hotta. Orbital ordering phenomena in d-and f-electron systems. *Reports on Progress in Physics*, 69(7):2061, 2006.
- [28] Shuxiang Zhou, Hao Ma, et al. Capturing the ground state of uranium dioxide from first principles: Crystal distortion, magnetic structure, and phonons. *Physical Review B*, 106(12):125134, 2022.
- [29] Ryousuke Shiina. Mechanism of non-coplanar magnetic ordering assisted by the jahn–teller effect in  $\text{UO}_2$ . *Journal of the Physical Society of Japan*, 91(2):023704, 2022.
- [30] Judy WL Pang, William JL Buyers, Aleksandr Chernatynskiy, Mark D Lumsden, Bennett C Larson, and Simon R Phillpot. Phonon lifetime investigation of anharmonicity and thermal conductivity of  $\text{UO}_2$  by neutron scattering and theory. *Physical review letters*, 110(15):157401, 2013.
- [31] Xiao-Dong Wen, Richard L Martin, Thomas M Henderson, and Gustavo E Scuseria. Density functional theory studies of the electronic structure of solid state actinide oxides. *Chemical reviews*, 113(2):1063–1096, 2013.
- [32] James T Pegg, Ashley E Shields, Mark T Storr, Andrew S Wills, David O Scanlon, and Nora H de Leeuw. Hidden magnetic order in plutonium dioxide nuclear fuel. *Physical Chemistry Chemical Physics*, 20(32):20943–20951, 2018.
- [33] GM Kalvius, SL Ruby, BD Dunlap, GK Shenoy, D Cohen, and MB Brodsky. Mössbauer isomer shift in  $^{243}\text{Am}$ . *Physics Letters B*, 29(8):489–490, 1969.
- [34] A Bœuf, JM Fournier, Jean-François Gueugnon, L Manes, J Rebizant, and F Rustichelli. Neutron diffrac-

- tion study of  $^{243}\text{AmO}_2$ . *Journal de Physique Lettres*, 40(14):335–338, 1979.
- [35] JC Lashley, A Lawson, RJ McQueeney, and GH Lander. Absence of magnetic moments in plutonium. *Physical Review B*, 72(5):054416, 2005.
- [36] GR Stewart. Non-fermi-liquid behavior in  $d$ - and  $f$ -electron metals. *Reviews of modern Physics*, 73(4):797, 2001.
- [37] Christian Pfleiderer. Superconducting phases of  $f$ -electron compounds. *Reviews of Modern Physics*, 81(4):1551, 2009.
- [38] John A Mydosh and Peter M Oppeneer. Colloquium: Hidden order, superconductivity, and magnetism: The unsolved case of  $\text{URu}_2\text{Si}_2$ . *Reviews of Modern Physics*, 83(4):1301, 2011.
- [39] M Brian Maple, Ryan E Baumbach, Nicholas P Butch, James J Hamlin, and Marc Janoschek. Non-fermi liquid regimes and superconductivity in the low temperature phase diagrams of strongly correlated  $d$ - and  $f$ -electron materials. *Journal of Low Temperature Physics*, 161(1):4–54, 2010.
- [40] Kevin D Vallejo, Firoza Kabir, Narayan Poudel, Chris Marianetti, David H Hurley, Paul Simmonds, Cody A Dennett, and Krzysztof Gofryk. Advances in actinide thin films: synthesis, properties, and future directions. *Reports on Progress in Physics*, 2022.
- [41] David H Hurley, Anter El-Azab, Matthew S Bryan, Michael WD Cooper, Cody A Dennett, Krzysztof Gofryk, Lingfeng He, Marat Khafizov, Gerard H Lander, Michael E Manley, et al. Thermal energy transport in oxide nuclear fuel. *Chemical Reviews*, 122(3):3711–3762, 2021.
- [42] Russell E Walstedt, Yo Tokunaga, and Shinsaku Kambe. NMR studies of actinide oxides—a review. *Comptes Rendus Physique*, 15(7):563–572, 2014.
- [43] Laura Martel, Nicola Magnani, Jean-Francois Vigier, Jacobus Boshoven, Chris Selfslag, Ian Farnan, Jean-Christophe Griveau, Joseph Somers, and Thomas Fanghänel. High-resolution solid-state oxygen-17 NMR of actinide-bearing compounds: an insight into the  $5f$  chemistry. *Inorganic chemistry*, 53(13):6928–6933, 2014.
- [44] Wei-Qun Shi, Li-Yong Yuan, Cong-Zhi Wang, Lin Wang, Lei Mei, Cheng-Liang Xiao, Li Zhang, Zi-Jie Li, Yu-Liang Zhao, and Zhi-Fang Chai. Exploring actinide materials through synchrotron radiation techniques. *Advanced Materials*, 26(46):7807–7848, 2014.
- [45] Lindsay E Roy. Electronic structure of actinide oxides. *The Heaviest Metals: Science and Technology of the Actinides and Beyond*, page 123, 2019.
- [46] Yurii A Teterin and Anton Yu Teterin. The structure of x-ray photoelectron spectra of light actinide compounds. *Russian chemical reviews*, 73(6):541–580, 2004.
- [47] RG Haire and L Eyring. Comparisons of the binary oxides. *Handbook on the Physics and Chemistry of Rare Earths*, 18:413–505, 1994.
- [48] Lester R Morss. Synthesis of actinide oxides. In *Synthesis of Lanthanide and Actinide Compounds*, pages 237–258. Springer, 1991.
- [49] Joseph J Katz. *The Chemistry of the Actinide and Transactinide Elements (Volumes 1-5)*, volume 1. Springer Science & Business Media, 2007.
- [50] Song Qi, Fang Guan, Dan Peng, Xuyi Zhang, and Wuping Liao. A simple method for preparing  $\text{ThO}_2$  ceramics with high density. *International Journal of Applied Ceramic Technology*, 2022.
- [51] SE Nave, RG Haire, and Paul G Huray. Magnetic properties of actinide elements having the  $5f^6$  and  $5f^7$  electronic configurations. *Physical Review B*, 28(5):2317, 1983.
- [52] OA Vita, CR Walker, and E Litteral. The gravimetric determination of uranium in uranyl nitrate. *Analytica Chimica Acta*, 64(2):249–257, 1973.
- [53] K Richter and C Sari. Phase relationships in the neptunium-oxygen system. *Journal of Nuclear Materials*, 148(3):266–271, 1987.
- [54] R.D. Baybarz and R.G. Haire. Investigation of the transplutonium oxides by x ray and electron diffraction. Technical report, Divison of Technical Information Extension, U.S. Atomic Energy Commission, jan 1972.
- [55] RG Wymer and JH Coobs. Preparation, coating, evaluation, and irradiation testing of sol-gel oxide microspheres. Technical report, Oak Ridge National Lab., Tenn., 1965.
- [56] YM Kulyako, SA Perevalov, TI Trofimov, DA Malikov, SE Vinokurov, MD Samsonov, BF Myasodov, AM Fedoseev, AA Bessonov, and AY Shadrin.  $\text{UO}_2$ ,  $\text{NpO}_2$  and  $\text{PuO}_2$  preparation in aqueous nitrate solutions in the presence of hydrazine hydrate. *Journal of Radioanalytical and Nuclear Chemistry*, 299(3):1293–1298, 2014.
- [57] Séverine Planteur, M Bertrand, E Plasari, B Courtaud, and JP Gaillard. Crystal growth kinetics of the uranium peroxide. *Procedia Chemistry*, 7:725–730, 2012.
- [58] Kevin E Roberts, Thomas J Wolery, Cynthia E Atkins-Duffin, Traudel G Prussin, Patrick G Allen, Jerome J Bucher, David K Shuh, Robert J Finch, and Stanley G Prussin. Precipitation of crystalline neptunium dioxide from near-neutral aqueous solution. *Radiochimica Acta*, 91(2):87–92, 2003.
- [59] IS Kurina, LS Gudkov, and VN Rumyantsev. Investigation of  $\text{ThO}_2$  and  $(\text{U}, \text{Th})\text{O}_2$ . *Atomic Energy*, 92(6):461–467, 2002.
- [60] RB Matthews. Thoria sol-gel processes. Technical report, Atomic Energy of Canada Ltd., 1978.
- [61] Claude C Herrick and Robert G Behrens. Growth of large uraninite and thorianite single crystal from the melt using a cold-crucible technique. *Journal of Crystal Growth*, 51(2):183–189, 1981.
- [62] CB Finch and G Wayne Clark. Single-crystal growth of thorium dioxide from lithium ditungstate solvent. *Journal of Applied Physics*, 36(7):2143–2145, 1965.
- [63] BM Wanklyn and BJ Garrard. The flux growth of large thoria and ceria crystals. *Journal of crystal growth*, 66(2):346–350, 1984.
- [64] GD Andreotti, G Calestani, A Montenero, and M Bettinelli. Crystal growth from the system  $\text{ThO}_2\text{-PbO-V}_2\text{O}_5$ . *Journal of crystal growth*, 71(2):289–294, 1985.
- [65] G Garton, SH Smith, and Barbara M Wanklyn. Crystal growth from the flux systems  $\text{PbO-V}_2\text{O}_5$  and  $\text{Bi}_2\text{O}_3\text{-V}_2\text{O}_5$ . *Journal of Crystal Growth*, 13:588–592, 1972.
- [66] C Rizzoli and JC Spirlet. Single crystal growth of actinide dioxides. *Inorganica Chimica Acta*, 94(1-3):112–113, 1984.
- [67] Robert C Linares. Growth and properties of  $\text{CeO}_2$  and  $\text{ThO}_2$  single crystals. *Journal of Physics and Chemistry of Solids*, 28(7):1285–1291, 1967.

- [68] AB Chase and Judith A Osmer. Synthesis of thorianite crystals from bismuth oxide-lead fluoride melts. *American Mineralogist: Journal of Earth and Planetary Materials*, 49(9-10):1469–1471, 1964.
- [69] Matthew Mann, Daniel Thompson, Karn Serivalsatit, Terry M Tritt, John Ballato, and Joseph Kolis. Hydrothermal growth and thermal property characterization of  $\text{ThO}_2$  single crystals. *Crystal growth & design*, 10(5):2146–2151, 2010.
- [70] Jacob Castilow, Timothy W Zens, J Matthew Mann, Joseph W Kolis, Colin D McMillen, and James Petrosky. Hydrothermal synthesis and characterization of  $\text{ThO}_2$ ,  $\text{U}_x\text{Th}_{1-x}\text{O}_2$ , and  $\text{UO}_x$ . *MRS Online Proceedings Library (OPL)*, 1576, 2013.
- [71] TS Laszlo, PaulJ Sheehan, and RichardE Gannon. Thoria single crystals grown by vapor deposition in a solar furnace. *Journal of Physics and Chemistry of Solids*, 28(2):313–316, 1967.
- [72] Katsuhiko Kawabuchi and Saburo Magari. Deposition of crystals from the plasmas of  $\text{ZrO}_2$ ,  $\text{HfO}_2$ ,  $\text{ThO}_2$ , and  $\text{CeO}_2$ . *Journal of Applied Physics*, 50(10):6222–6229, 1979.
- [73] Katsuhiko Kawabuchi and Saburo Magari. Growth morphology of  $\text{UO}_2$ ,  $\text{ZrO}_2$ ,  $\text{HfO}_2$  and  $\text{ThO}_2$  crystallites grown from oxide plasmas. *Journal of Crystal Growth*, 49(1):81–84, 1980.
- [74] Philip A Sellers, Sherman Fried, Robert E Elson, and WH Zachariasen. The preparation of some protactinium compounds and the metal. *Journal of the American Chemical Society*, 76(23):5935–5938, 1954.
- [75] T Stchouzkoy, R MUXART, G Bouissieres, and H PEZERAT. Contribution a letude des oxydes de protactinium. *COMPTEs RENDUS HEBDOMADAIRES DES SEANCES DE L ACADEMIE DES SCIENCES*, 259(18):3016, 1964.
- [76] HW Kirby. Calorimetric determination of the half-life of protactinium-231. *Journal of Inorganic and Nuclear Chemistry*, 18:8–12, 1961.
- [77] OK Tallent and LM Ferris. Equilibrium precipitation of protactinium oxide from molten  $\text{LiF-BeF}_2\text{-ThF}_4\text{-UF}_4\text{-PaF}_5$  mixtures between 535 and 670 c. Technical report, Oak Ridge National Lab., TN, 1974.
- [78] Jack Belle. *Uranium dioxide: properties and nuclear applications*, volume 4. Naval Reactors, Division of Reactor Development, US Atomic Energy Commission, 1961.
- [79] Shōichi Nasu. Preparation of single crystals of  $\text{UO}_2$  by sintering. *Japanese Journal of Applied Physics*, 3(10):664, 1964.
- [80] Takemaro Sakurai, Osama Kamada, and Mareo Ishigame. Uranium dioxide crystals grown by a solar furnace. *Journal of Crystal Growth*, 2(5):326–327, 1968.
- [81] AT Chapman and GW Clark. Growth of  $\text{UO}_2$  single crystals using the floating-zone technique. *J. Amer. Ceram. Soc.*, 48(ORNL-P-1279), 1965.
- [82] M Schlechter. The preparation of crystalline  $\text{UO}_2$  by thermal decomposition of  $\text{UOCl}_2$  dissolved in molten  $\text{UCl}_4$ . *Journal of Nuclear Materials*, 28(2):228–229, 1968.
- [83] RG Robins. Uranium dioxide single crystals by electrodeposition. *Journal of Nuclear Materials*, 3(3):294–301, 1961.
- [84] Yuhe Li, Wei Huang, and Qingnuan Li. Studies on the electrodeposition of  $\text{uo}_2$  production in  $\text{uo}_2\text{cl}_2\text{-licl-kcl}$  melt. *Journal of The Electrochemical Society*, 169(4):042505, 2022.
- [85] S Amelinckx, J Bressers, K Nevelsteen, E Smets, and W Van Lierde. Growth of  $\text{UO}_2$  single crystals. Technical Report 693, European Atomic Energy Community - EURATOM, 1963.
- [86] Karl Rickert, Michael A Velez, Timothy A Prusnick, David B Turner, Martin M Kimani, Thomas Bowen, and J Matthew Mann. Hydrothermal crystal growth on non-native substrates: The case of  $\text{UO}_2$ . *Crystal Growth & Design*, 21(11):6289–6300, 2021.
- [87] Christopher Young, James Petrosky, J Matthew Mann, Eric M Hunt, David Turner, and Tony Kelly. The work function of hydrothermally synthesized  $\text{UO}_2$  and the implications for semiconductor device fabrication. *physica status solidi (RRL)–Rapid Research Letters*, 10(9):687–690, 2016.
- [88] Christina L Dugan, George Glenn Peterson, Alyssa Mock, Christopher Young, J Matthew Mann, Michael Nastasi, Mathias Schubert, Lu Wang, Wai-Ning Mei, Iori Tanabe, et al. Electrical and material properties of hydrothermally grown single crystal (111)  $\text{UO}_2$ . *The European Physical Journal B*, 91(4):1–7, 2018.
- [89] Keiji Naito, Naoki Kamegashira, and Yuji Nomura. Single crystals of uranium oxides by chemical transport reactions. *Journal of Crystal Growth*, 8(2):219–220, 1971.
- [90] Samuel P Faile. Growth of uranium dioxide crystals using tellurium tetrachloride and argon. *Journal of Crystal Growth*, 43(1):133–134, 1978.
- [91] RN Singh and RL Coble. Growth of uranium dioxide single crystals by chemical vapor deposition. *Journal of Crystal Growth*, 21(2):261–266, 1974.
- [92] J Spirlet, E Bednarczyk, I Ray, and W Müller. Crystal growth of actinide dioxides by chemical transport. *Le Journal de Physique Colloques*, 40(C4):C4–108, 1979.
- [93] W Van Lierde, R Strumane, E Smets, and S Amelinckx. The preparation of uranium oxide single crystals by sublimation. *Journal of Nuclear Materials*, 5(2):250–253, 1962.
- [94] Aurélien Soulié, Gianguido Baldinozzi, Frédéric Garrido, and Jean-Paul Crocombette. Clusters of oxygen interstitials in  $\text{UO}_{2+x}$  and  $\alpha\text{-U}_4\text{O}_9$ : Structure and arrangements. *Inorganic Chemistry*, 58(19):12678–12688, 2019.
- [95] Darrell W Osborne, Edgar F Westrum Jr, and Harold R Lohr. The heat capacity and thermodynamic functions of tetrauranium nonoxide from 5 to 310° k. *Journal of the American Chemical Society*, 79(3):529–530, 1957.
- [96] NORIO Masaki et al. Analysis of the superstructure of  $\text{U}_4\text{O}_9$  by neutron diffraction. *Acta Crystallographica Section B: Structural Crystallography and Crystal Chemistry*, 28(3):785–791, 1972.
- [97] Gregory Leinders, René Bes, Kristina O Kvashnina, and Marc Verwerft. Local structure in u (IV) and u (v) environments: The case of  $\text{U}_3\text{O}_7$ . *Inorganic chemistry*, 59(7):4576–4587, 2020.
- [98] Lionel Desgranges, Gianguido Baldinozzi, Gurvan Rousseau, Jean-Claude Niepce, and Gilbert Calvarin. Neutron diffraction study of the in situ oxidation of  $\text{UO}_2$ . *Inorganic chemistry*, 48(16):7585–7592, 2009.
- [99] N Masaki and T Ishii. The preparation of  $\text{U}_4\text{O}_9$  single crystal. *Journal of Crystal Growth*, 6(2):207–209, 1970.
- [100] HR Hoekstra, A Santoro, and S Siegel. The low temperature oxidation of  $\text{UO}_2$  and  $\text{U}_4\text{O}_9$ . *Journal of Inorganic and Nuclear Chemistry*, 18:166–178, 1961.

- [101] DJM Bevan, IE Grey, and BTM Willis. The crystal structure of  $\beta$ - $\text{U}_4\text{O}_9$ -y. *Journal of Solid State Chemistry*, 61(1):1–7, 1986.
- [102] Edgar F Westrum Jr and F Grønvold. Triuranium heptaoxides: Heat capacities and thermodynamic properties of  $\alpha$ - and  $\beta$ - $\text{U}_3\text{O}_7$  from 5 to 350 k. *Journal of Physics and Chemistry of Solids*, 23(1-2):39–53, 1962.
- [103] Geoffrey C Allen and Jonathan W Tyler. Surface characterisation of  $\beta$ - $\text{U}_3\text{O}_7$  using x-ray photoelectron spectroscopy. *Journal of the Chemical Society, Faraday Transactions 1: Physical Chemistry in Condensed Phases*, 82(5):1367–1379, 1986.
- [104] F Garrido, RM Ibberson, L Nowicki, and BTM Willis. Cuboctahedral oxygen clusters in  $\text{U}_3\text{O}_7$ . *Journal of nuclear materials*, 322(1):87–89, 2003.
- [105] Henry R Hoekstra, Stanley Siegel, and Francis X Gallagher. The uranium-oxygen system at high pressure. *Journal of Inorganic and Nuclear Chemistry*, 32(10):3237–3248, 1970.
- [106] I SPITSYN, TSVIGUNO. AN, LM Kovba, and KUZMICHE. EU. Study of phase-transitions in uranium oxides. *DOKLADY AKADEMII NAUK SSSR*, 204(3):640, 1972.
- [107] RE Rundle, NC Baenziger, AS Wilson, and RA McDonald. The structures of the carbides, nitrides and oxides of uranium. *Journal of the American Chemical Society*, 70(1):99–105, 1948.
- [108] Lénaïc Desfougeres, Eleonore Welcomme, Maelig Olivier, Philippe M Martin, Julie Hennuyer, Myrtille OJY Hunault, Renaud Podor, Nicolas Clavier, and Loïc Favregeon. Oxidation as an early stage in the multistep thermal decomposition of uranium (IV) oxalate into  $\text{U}_3\text{O}_8$ . *Inorganic Chemistry*, 59(12):8589–8602, 2020.
- [109] Kun Woo Song, Keon Sik Kim, Ki Won Kang, and Youn Ho Jung. Fabrication of large-grained  $\text{UO}_2$  pellets by the addition of  $\text{U}_3\text{O}_8$  seeds. *Journal of Nuclear Science and Technology*, 39(sup3):838–841, 2002.
- [110] BO Loopstra. The phase transition in  $\alpha$ - $\text{U}_3\text{O}_8$  at 210 c. *Journal of Applied Crystallography*, 3(2):94–96, 1970.
- [111] FX Zhang, Maik Lang, JW Wang, WX Li, K Sun, V Prakashpenka, and Rodney C Ewing. High-pressure  $\text{U}_3\text{O}_8$  with the fluorite-type structure. *Journal of Solid State Chemistry*, 213:110–115, 2014.
- [112] RG Robins. Twinning, slip and cleavage in  $\text{U}_3\text{O}_8$ . *Journal of Nuclear Materials*, 5(3):301–307, 1962.
- [113] BO Loopstra. The structure of  $\beta$ - $\text{U}_3\text{O}_8$ . *Acta Crystallographica Section B: Structural Crystallography and Crystal Chemistry*, 26(5):656–657, may 1970.
- [114] HR Hoekstra, S Siegel, LH Fuchs, and JJ Katz. The uranium–oxygen system:  $\text{UO}_{2.5}$  to  $\text{U}_3\text{O}_8$ . *The Journal of Physical Chemistry*, 59(2):136–138, 1955.
- [115] VJ Wheeler, RM Dell, and E Wait. Uranium trioxide and the  $\text{UO}_3$  hydrates. *Journal of Inorganic and Nuclear Chemistry*, 26(11):1829–1845, 1964.
- [116] Lucas E Sweet, Thomas A Blake, Charles H Henager, Shenyang Hu, Timothy J Johnson, David E Meier, Shane M Peper, and Jon M Schwantes. Investigation of the polymorphs and hydrolysis of uranium trioxide. *Journal of Radioanalytical and Nuclear Chemistry*, 296(1):105–110, 2013.
- [117] C t Greaves and BEF Fender. The structure of  $\alpha$ - $\text{UO}_3$  by neutron and electron diffraction. *Acta Crystallographica Section B: Structural Crystallography and Crystal Chemistry*, 28(12):3609–3614, 1972.
- [118] BH Kim, YB Lee, MA Prelas, and TK Ghosh. Thermal and x-ray diffraction analysis studies during the decomposition of ammonium uranyl nitrate. *Journal of radio-analytical and nuclear chemistry*, 292:1075–1083, 2012.
- [119] Erich Heinz Pieter Cordfunke.  $\alpha$ - $\text{UO}_3$ : Its preparation and thermal stability. *Journal of Inorganic and Nuclear Chemistry*, 23(3-4):285–286, 1961.
- [120] Irving Sheft, Sherman Fried, and Norman Davidson. Preparation of uranium trioxide. *Journal of the American Chemical Society*, 72(5):2172–2173, 1950.
- [121] PC Debets. The structure of  $\beta$ - $\text{UO}_3$ . *Acta Crystallographica*, 21(4):589–593, 1966.
- [122] Tyler L Spano, Ashley E Shields, Brodie Barth, Jeremiah D Gruidl, Jennifer L Niedziela, Roger J Kapsimalis, and Andrew Miskowicz. Computationally guided investigation of the optical spectra of pure  $\beta$ - $\text{UO}_3$ . *Inorganic Chemistry*, 59(16):11481–11492, 2020.
- [123] RWPM de Engmann and PM De Wolf. The crystal structure of  $\gamma$ - $\text{UO}_3$ . *Acta Crystallographica*, 16(10):993–996, 1963.
- [124] H Hoekstra, S Siegel, and E Gebert. On the unit cell of  $\gamma$ - $\text{UO}_3$ . *Journal of Inorganic and Nuclear Chemistry*, 28(9):2065–2066, 1966.
- [125] E Wait. A cubic form of uranium trioxide. *Journal of Inorganic and Nuclear Chemistry*, 1(4-5):309–312, 1955.
- [126] MT Weller, PG Dickens, and DJ Penny. The structure of  $\delta$ - $\text{UO}_3$ . *Polyhedron*, 7(3):243–244, 1988.
- [127] JJ Katz and DM Gruen. Higher oxides of the actinide elements. the preparation of  $\text{Np}_3\text{O}_8$ . *Journal of the American Chemical Society*, 71(6):2106–2112, 1949.
- [128] Tyler L Spano, Rodney Hunt, Roger J Kapsimalis, Jennifer L Niedziela, Ashley E Shields, and Andrew Miskowicz. Optical vibrational spectra and proposed crystal structure of  $\varepsilon$ - $\text{UO}_3$ . *Journal of Nuclear Materials*, 559:153386, 2022.
- [129] Stephen L Yarbrow, Sharon L Dunn, and Stephen B Schreiber. Preparation of pure neptunium oxide for nondestructive assay standards. Technical report, Los Alamos National Lab., NM (USA), 1991.
- [130] AA Bessonov, TV Afonova, and NN Krot. On formation of neptunium (5) and (6) during thermal decomposition of neptunium (4) compounds. *Radiokhimiya*, 31(5):9–13, 1989.
- [131] JA Fahey, RP Turcotte, and TD Chikalla. Thermal expansion of the actinide dioxides. *Inorganic and Nuclear Chemistry Letters*, 10(6):459–465, 1974.
- [132] KW Bagnall and JB Laidler. 516. neptunium and plutonium trioxide hydrates. *Journal of the Chemical Society (Resumed)*, pages 2693–2696, 1964.
- [133] CB Finch and GW Clark. High-temperature solution growth of single-crystal neptunium dioxide. *Journal of Crystal Growth*, 6(3):245–248, 1970.
- [134] L Martinot, A Machiels, J Fuger, and G Duyckaerts. Electrochemical growth of  $\text{NpO}_2$  single crystals. *Bulletin des Sociétés Chimiques Belges*, 79(1-2):125–131, 1970.
- [135] Dai Aoki, Yoshiya Homma, Hironori Sakai, Shugo Ikeda, Yoshinobu Shiokawa, Etsuji Yamamoto, Akio Nakamura, Yoshinori Haga, and Yoshichika Ōnuki. Single crystal growth and magnetic properties of neptunium compounds. *Journal of the Physical Society of Japan*, 75(Suppl):36–38, 2006.
- [136] JC Spirlet, E Bednarczyk, J Rebizant, and CT Walker. Préparation de monocristaux de dioxyde de neptunium

- par transport chimique en phase gazeuse. *Journal of Crystal Growth*, 49(1):171–172, 1980.
- [137] L Merli and J Fuger. Thermochemistry of a few neptunium and neodymium oxides and hydroxides. *Radiochimica Acta*, 66(s1):109–114, 1994.
- [138] Donald Cohen and AJ Walter. 517. neptunium pentoxide. *Journal of the Chemical Society (Resumed)*, pages 2696–2699, 1964.
- [139] Donald Cohen. Oxides of neptunium (v) and neptunium (vi) from molten salts. *Inorganic Chemistry*, 2(4):866–867, 1963.
- [140] H Nitsche, RC Gatti, and EM Standifer. Measured solubilities and speciations of neptunium, plutonium, and americium in a typical groundwater (j-13) from the yucca mountain region. Technical report, Los Alamos National Lab., 1993.
- [141] Tori Z Forbes, Peter C Burns, S Skanthakumar, and L Soderholm. Synthesis, structure, and magnetism of  $\text{Np}_2\text{O}_5$ . *Journal of the American Chemical Society*, 129(10):2760–2761, 2007.
- [142] Howard E Flotow and Marvin Tetenbaum. Heat capacity and thermodynamic functions of  $\beta$ - $^{242}\text{Pu}_2\text{O}_3$  from 8 to 350 k. contributions to the excess entropy. *The Journal of Chemical Physics*, 74(9):5269–5277, 1981.
- [143] TD Chikalla, CE McNeilly, and RE Skavdahl. The plutonium-oxygen system. *Journal of Nuclear Materials*, 12(2):131–141, 1964.
- [144] JL Drummond and GA Welch. 964. the preparation and properties of some plutonium compounds. part vi. plutonium dioxide. *Journal of the Chemical Society (Resumed)*, pages 4781–4785, 1957.
- [145] Howard E Flotow, Darrell W Osborne, Sherman M Fried, and John G Malm. Heat capacity of  $^{242}\text{PuO}_2$  from 12 to 350 K and of  $^{244}\text{PuO}_2$  from 4 to 25 k. entropy, enthalpy, and gibbs energy of formation of  $\text{PuO}_2$  at 298.15 k. *The Journal of Chemical Physics*, 65(3):1124–1129, 1976.
- [146] DL Plymale and WH Smith. The preparation of  $^{238}\text{Pu}$  dioxide microspheres by the sol-gel process. Technical report, Mound Lab., Miamisburg, Ohio, 1967.
- [147] MH Lloyd and RG Haire. A sol-gel process for preparing dense forms of  $\text{PuO}_2$ . *Nuclear Applications*, 5(3):114–122, 1968.
- [148] A Modin, SM Butorin, J Vegelius, Anders Olsson, C-J Englund, J Andersson, L Werme, J Nordgren, Tanel Käambre, Gunnar Skarnemark, et al. Closed source experimental system for soft x-ray spectroscopy of radioactive materials. *Review of scientific instruments*, 79(9):093103, 2008.
- [149] CB Finch and GW Clark. High-temperature solution growth of single-crystal plutonium dioxide. *Journal of Crystal Growth*, 12(2):181–182, 1972.
- [150] M Schlechter. The preparation of  $\text{PuO}_2$  crystals by thermal decomposition of  $\text{Pu}(\text{SO}_4)_2$  dissolved in chloride melts. *Journal of Nuclear Materials*, 37(1):82–88, 1970.
- [151] J Rebizant, E Bednarczyk, P Boulet, C Fuchs, and F Wastin. Single crystal growth of  $(\text{U}_{1-x}\text{Pu}_x)\text{O}_2$  mixed oxides. In *AIP Conference Proceedings*, volume 532, pages 355–356. American Institute of Physics, 2000.
- [152] KD Phipps and DB Sullenger. Plutonium dioxide: preparation of single crystals. *Science*, 145(3636):1048–1049, 1964.
- [153] Lester R Morss and David C Sonnenberger. Enthalpy of formation of americium sesquioxide; systematics of actinide sesquioxide thermochemistry. *Journal of Nuclear Materials*, 130:266–272, 1985.
- [154] Lohr Eyring, HR Lohr, and BB Cunningham. Heats of reaction of some oxides of americium and praseodymium with nitric acid and an estimate of the potentials of the am (III)—am (IV) and pr (III)—pr (IV) couples. *Journal of the American Chemical Society*, 74(5):1186–1190, 1952.
- [155] C Hurtgen and J Fuger. Self-irradiation effects in americium oxides. *Inorganic and Nuclear Chemistry Letters*, 13(3-4):179–188, 1977.
- [156] RD Baybarz. *Preparation of americium dioxide by thermal decomposition of americium oxalate in air*. Oak Ridge National Laboratory, 1960.
- [157] LR Morss and J Fuger. Enthalpy formation of americium dioxide and a thermochemical estimate of the electrode potential  $\text{Am}^{4+}/\text{Am}^{3+}$ . *Journal of Inorganic and Nuclear Chemistry*, 43(9):2059–2064, 1981.
- [158] M Noé, J Fuger, and G Duyckaerts. Some recent observations on curium sesquioxide. *Inorganic and Nuclear Chemistry Letters*, 6(1):111–119, 1970.
- [159] LR Morss, J Fuger, J Goffart, and RG Haire. Enthalpy of formation and magnetic susceptibility of curium sesquioxide,  $\text{Cm}_2\text{O}_3$ . *Inorganic Chemistry*, 22(14):1993–1996, 1983.
- [160] LB Asprey, FH Ellinger, S Fried, and WH Zachariasen. Evidence for quadrivalent curium: X-ray data on curium oxides1. *Journal of the American Chemical Society*, 77(6):1707–1708, 1955.
- [161] John C Posey. Curium-244 isotopic power fuel: chemical recovery from commercial power reactor fuels. Technical report, Oak Ridge National Lab., Tenn.(USA), 1973.
- [162] Hermann O Haug. Curium sesquioxide  $\text{Cm}_2\text{O}_3$ . *Journal of Inorganic and Nuclear Chemistry*, 29(11):2753–2758, 1967.
- [163] M Noé and J Fuger. Self-radiation effects on the lattice parameter of  $^{244}\text{CmO}_2$ . *Inorganic and Nuclear Chemistry Letters*, 7(5):421–430, 1971.
- [164] William H Hale Jr and WC Mosley. Preparation of curium oxysulfate and curium oxide by resin calcination. *Journal of Inorganic and Nuclear Chemistry*, 35(1):165–171, 1973.
- [165] JR Peterson and J Fuger. The dioxide of  $^{248}\text{Cm}$ . *Journal of Inorganic and Nuclear Chemistry*, 33(12):4111–4117, 1971.
- [166] RP Turcotte, TD Chikalla, RG Haire, and JA Fahey. Phase behaviour in the berkelium-oxygen system. *Journal of Inorganic and Nuclear Chemistry*, 42(12):1729–1733, 1980.
- [167] JR Peterson and BB Cunningham. Crystal structures and lattice parameters of the compounds of berkelium. i. berkelium dioxide and cubic berkelium sesquioxide. 1967.
- [168] RD Baybarz. The berkelium oxide system. *Journal of Inorganic and Nuclear Chemistry*, 30(7):1769–1773, 1968.
- [169] RD Baybarz, RG Haire, and JA Fahey. On the californium oxide system. *Journal of Inorganic and Nuclear Chemistry*, 34(2):557–565, 1972.
- [170] Lester R Morss, J Fuger, J Goffart, N Edelstein, and GV Shalimoff. Enthalpy of formation and magnetic susceptibility of californium sesquioxide,  $\text{Cf}_2\text{O}_3$ . *Journal of*

- the Less Common Metals*, 127:251–257, 1987.
- [171] Rod Joseph McEachern and P Taylor. A review of the oxidation of uranium dioxide at temperatures below 400 c. *Journal of Nuclear Materials*, 254(2-3):87–121, 1998.
- [172] John Emsley. Nature’s building blocks hardcover, 2001.
- [173] D. W. Brite and H. J. Anderson. Meeting on characterization of uranium dioxide; tid-7637. Technical report, Oak Ridge National Lab., Tenn., 1961.
- [174] Christian A Juillerat, Vladislav V Klepov, Gregory Morrison, Kristen A Pace, and Hans-Conrad Zur Loye. Flux crystal growth: a versatile technique to reveal the crystal chemistry of complex uranium oxides. *Dalton Transactions*, 48(10):3162–3181, 2019.
- [175] Vladislav V Klepov, Christian A Juillerat, Kristen A Pace, Gregory Morrison, and Hans-Conrad Zur Loye. “soft” alkali bromide and iodide fluxes for crystal growth. *Frontiers in Chemistry*, 8:518, 2020.
- [176] Kang Wang, Xiao-Li Hu, Xiao Li, Zhong-Min Su, and En-Long Zhou. Solvent induced two Cd-MOFs as luminescent sensors for picric acid,  $\text{Fe}^{3+}$  and  $\text{Cr}_2\text{O}_7^{2-}$ . *Journal of Solid State Chemistry*, 298:122128, 2021.
- [177] Daniel E Bugaris and Hans-Conrad zur Loye. Materials discovery by flux crystal growth: quaternary and higher order oxides. *Angewandte chemie international edition*, 51(16):3780–3811, 2012.
- [178] Colin D McMillen and Joseph W Kolis. Bulk single crystal growth from hydrothermal solutions. *Philosophical Magazine*, 92(19-21):2686–2711, 2012.
- [179] Karin Popa, Olaf Walter, Oliver Dieste Blanco, Antony Guiot, Daniel Bouëxière, Jean-Yves Colle, Laura Martel, Mohamed Naji, and Dario Manara. A low-temperature synthesis method for  $\text{AnO}_2$  nanocrystals ( $\text{An} = \text{Th}, \text{U}, \text{Np}, \text{and Pu}$ ) and associate solid solutions. *CrystEngComm*, 20(32):4614–4622, 2018.
- [180] Richard Husar, René Hübner, Christoph Hennig, Philippe M Martin, Mélanie Chollet, Stephan Weiss, Thorsten Stumpf, Harald Zänker, and Atsushi Ikeda-Ohno. Intrinsic formation of nanocrystalline neptunium dioxide under neutral aqueous conditions relevant to deep geological repositories. *Chemical Communications*, 51(7):1301–1304, 2015.
- [181] Michael Binnewies, Robert Glaum, Marcus Schmidt, and Peer Schmidt. Chemical vapor transport reactions—a historical review. *Zeitschrift für anorganische und allgemeine Chemie*, 639(2):219–229, 2013.
- [182] Justin N Cross, Eric M Villa, Shuao Wang, Juan Diwu, Matthew J Polinski, and Thomas E Albrecht-Schmitt. Syntheses, structures, and spectroscopic properties of plutonium and americium phosphites and the redetermination of the ionic radii of pu (iii) and am (iii). *Inorganic Chemistry*, 51(15):8419–8424, 2012.
- [183] Travis K Deason, Gregory Morrison, Amir Mofrad, Hunter B Tisdale, Jake Amoroso, David DiPrete, Gary Was, Kai Sun, Theodore M Besmann, and Hans-Conrad Zur Loye. Developing waste forms for transuranic elements: Quaternary neptunium fluorides of the type  $\text{Na}_x\text{Mn}_m\text{Pu}_3\text{F}_{30}$  ( $m = \text{ti}, \text{v}, \text{cr}, \text{mn}, \text{fe}, \text{co}, \text{ni}, \text{al}, \text{ga}$ ). *Journal of the American Chemical Society*, 145(1):465–475, 2022.
- [184] Samantha K Cary, Monica Vasiliu, Ryan E Baumbach, Jared T Stritzinger, Thomas D Green, Kariem Diefenbach, Justin N Cross, Kenneth L Knappenberger, Guokui Liu, Mark A Silver, et al. Emergence of californium as the second transitional element in the actinide series. *Nature communications*, 6(1):6827, 2015.
- [185] Richard E Sykora, Zerihun Assefa, Richard G Haire, and Thomas E Albrecht-Schmitt. Hydrothermal synthesis, structure, raman spectroscopy, and self-irradiation studies of  $248\text{cm}(\text{io}3)$  3. *Journal of Solid State Chemistry*, 177(12):4413–4419, 2004.
- [186] Travis K Deason, Adrian T Hines, Gregory Morrison, Mark D Smith, Theodore M Besmann, Amir M Mofrad, Fernando F Fondeur, Ingrid Lehman-Andino, Jake W Amoroso, David P DiPrete, et al. Flux crystal growth of the extended structure pu (v) borate  $\text{Na}_2(\text{puo}_2)(\text{bo}_3)$ . *Journal of the American Chemical Society*, 145(18):10007–10014, 2023.
- [187] Kristen A Pace, Vladislav V Klepov, Matthew S Christian, Gregory Morrison, Travis K Deason, Ceren Kutahyali Aslani, Theodore M Besmann, David P Diprete, Jake W Amoroso, and Hans-Conrad Zur Loye. Targeting complex plutonium oxides by combining crystal chemical reasoning with density-functional theory calculations: the quaternary plutonium oxide  $\text{Cs}_2\text{Pu}_6\text{O}_{15}$ . *Chemical Communications*, 56(66):9501–9504, 2020.
- [188] Toshiyuki Yamashita, Noriko Nitani, Toshihide Tsuji, and Hirornitsu Inagaki. Thermal expansions of  $\text{NpO}_2$  and some other actinide dioxides. *Journal of Nuclear Materials*, 245(1):72–78, may 1997.
- [189] ER Gardner, TL Markin, and RS Street. The plutonium-oxygen phase diagram. *Journal of Inorganic and Nuclear Chemistry*, 27(3):541–551, 1965.
- [190] J.P. Dancausse, R.G. Haire, S. Heathman, and U. Benedict. High-Pressure X-ray Diffraction Studies of Americium and Curium Dioxides. *Journal of Nuclear Science and Technology*, 39(sup3):136–139, nov 2002.
- [191] Denis Horlait, Richard Caraballo, Florent Lebreton, Christophe Jégou, Pascal Roussel, and Thibaud Delahaye. Self-irradiation and oxidation effects on americium sesquioxide and Raman spectroscopy studies of americium oxides. *Journal of Solid State Chemistry*, 217:159–168, sep 2014.
- [192] TD Chikalla and L Eyring. Phase relationships in the americium-oxygen system. *Journal of Inorganic and Nuclear Chemistry*, 30(1):133–145, 1968.
- [193] LR Morss, JW Richardson Jr, CW Williams, GH Lander, AC Lawson, NM Edelstein, and GV Shalimoff. Powder neutron diffraction and magnetic susceptibility of  $^{248}\text{CmO}_2$ . *Journal of the Less Common Metals*, 156(1-2):273–289, 1989.
- [194] W.C. Mosley. Phases and transformations in the curium-oxygen system. *Journal of Inorganic and Nuclear Chemistry*, 34(2):539–555, feb 1972.
- [195] JC Wallmann. A structural transformation of curium sesquioxide. *Journal of Inorganic and Nuclear Chemistry*, 26(12):2053–2057, 1964.
- [196] J.R. Peterson and B.B. Cunningham. Crystal structures and lattice parameters of the compounds of berkelium I. Berkelium dioxide and cubic berkelium sesquioxide. *Inorganic and Nuclear Chemistry Letters*, 3(9):327–336, sep 1967.
- [197] J.C. Copeland and B.B. Cunningham. Crystallography of the compounds of californium—II crystal structure and lattice parameters of californium oxychloride and californium sesquioxide. *Journal of Inorganic and Nuclear Chemistry*, 31(3):733–740, mar 1969.
- [198] J.C. Copeland. *PREPARATION AND CRYSTALLOGRAPHIC ANALYSIS OF CALIFORNIUM*

- SESQUIOXIDE AND CALIFORNIUM OXYCHLORIDE*. PhD thesis, University of California, Berkeley, 1967.
- [199] JL Green. *THE ABSORPTION SPECTRUM OF Cf<sup>β+</sup> AND CRYSTALLOGRAPHY OF CALIFORNIUM SESQUIOXIDE AND CALIFORNIUM TRICHLORIDE*. PhD thesis, University of California, Berkeley, Berkeley, CA, 1965.
- [200] Wingate A Lambertson, Melvin H Mueller, and FH Gunzel Jr. Uranium oxide phase equilibrium systems: Iv, uo<sub>2</sub>–tho<sub>2</sub>. *Journal of the American Ceramic Society*, 36(12):397–399, 1953.
- [201] Gregory Leinders, Thomas Cardinaels, Koen Binnemans, and Marc Verwerft. Accurate lattice parameter measurements of stoichiometric uranium dioxide. *Journal of Nuclear Materials*, 459:135–142, 2015.
- [202] Bert Onno Loopstra and Erich Heinz Pieter Cordfunke. On the structure of α-UO<sub>3</sub>. *Recueil des Travaux Chimiques des Pays-Bas*, 85(2):135–142, 1966.
- [203] Erik Enriquez, Gaoxue Wang, Yogesh Sharma, Ibrahim Sarpkaya, Qiang Wang, Di Chen, Nicholas Winner, Xiaofeng Guo, John Dunwoody, Joshua White, et al. Structural and optical properties of phase-pure UO<sub>2</sub>, α-U<sub>3</sub>O<sub>8</sub>, and α-UO<sub>3</sub> epitaxial thin films grown by pulsed laser deposition. *ACS Applied Materials & Interfaces*, 12(31):35232–35241, 2020.
- [204] BO Loopstra, JC Taylor, and AB Waugh. Neutron powder profile studies of the gamma uranium trioxide phases. *Journal of Solid State Chemistry*, 20(1):9–19, 1977.
- [205] S Siegel, H Hoekstra, and E Sherry. The crystal structure of high-pressure UO<sub>3</sub>. *Acta Crystallographica*, 20(2):292–295, 1966.
- [206] Jayangani I Ranasinghe, Linu Malakkal, Ericmoore Josson, Barbara Szpunar, and Jerzy A Szpunar. Comprehensive study on the electronic and optical properties of α-U<sub>3</sub>O<sub>8</sub>. *Computational Materials Science*, 171:109264, 2020.
- [207] Gregory Leinders, Janne Pakarinen, Rémi Delville, Thomas Cardinaels, Koen Binnemans, and Marc Verwerft. Low-temperature oxidation of fine UO<sub>2</sub> powders: A process of nanosized domain development. *Inorganic Chemistry*, 55(8):3915–3927, 2016.
- [208] LM Kovba, NI Komarevtseva, and EU Kuz'micheva. On the crystal structures of U<sub>13</sub>O<sub>34</sub> and delta-U<sub>2</sub>O<sub>5</sub>. *Radiokhimiya*, 21(5):754–757, 1979.
- [209] Lionel Desgranges, Gianguido Baldinozzi, David Simeone, and HE Fischer. Refinement of the α-U<sub>4</sub>O<sub>9</sub> crystalline structure: new insight into the U<sub>4</sub>O<sub>9</sub>→U<sub>3</sub>O<sub>8</sub> transformation. *Inorganic Chemistry*, 50(13):6146–6151, 2011.
- [210] K Ikushima, S Tsutsui, Y Haga, H Yasuoka, RE Walstedt, NM Masaki, A Nakamura, S Nasu, and Y Ōnuki. First-order phase transition in UO<sub>2</sub>: <sup>235</sup>U and <sup>17</sup>O NMR study. *Physical Review B*, 63(10):104404, 2001.
- [211] Yo Tokunaga, Tsuyoshi Nishi, Shinsaku Kambe, Masami Nakada, Yoshiya Homma, Hironori Sakai, and Hiroyuki Chudo. NMR study on AmO<sub>2</sub>: Comparison with UO<sub>2</sub> and NpO<sub>2</sub>. *Journal of the Physical Society of Japan*, 80(Suppl. A):SA110, 2011.
- [212] G Raphael and R Lallement. Susceptibilité magnétique de PuO<sub>2</sub>. *Solid State Communications*, 6(6):383–385, 1968.
- [213] Y Tokunaga, H Sakai, T Fujimoto, S Kambe, RE Walstedt, K Ikushima, H Yasuoka, D Aoki, Y Homma, Y Haga, et al. NMR studies of actinide dioxides. *Journal of alloys and compounds*, 444:241–245, 2007.
- [214] Bo Sun, Ping Zhang, and Xian-Geng Zhao. First-principles local density approximation+ u and generalized gradient approximation+ u study of plutonium oxides. *The Journal of chemical physics*, 128(8):084705, 2008.
- [215] Gérald Jomard, Bernard Amadon, Francois Bottin, and Marc Torrent. Structural, thermodynamic, and electronic properties of plutonium oxides from first principles. *Physical Review B*, 78(7):075125, 2008.
- [216] James T Pegg, Ashley E Shields, Mark T Storr, David O Scanlon, and Nora H De Leeuw. Noncollinear relativistic dft+ u calculations of actinide dioxide surfaces. *The Journal of Physical Chemistry C*, 123(1):356–366, 2018.
- [217] BC Frazer, G Shirane, DE Cox, and CE Olsen. Neutron-diffraction study of antiferromagnetism in UO<sub>2</sub>. *Physical Review*, 140(4A):A1448, 1965.
- [218] R Caciuffo, Giuseppe Amoretti, Paolo Santini, Gerard Heath Lander, J Kulda, and P de V Du Plessis. Magnetic excitations and dynamical jahn-teller distortions in uo 2. *Physical Review B*, 59(21):13892, 1999.
- [219] Boris Dorado, Gérald Jomard, Michel Freyss, and Marjorie Bertolus. Stability of oxygen point defects in UO<sub>2</sub> by first-principles DFT+U calculations: Occupation matrix control and jahn-teller distortion. *Physical Review B*, 82(3):035114, 2010.
- [220] Katsunori Kubo and Takashi Hotta. Magnetic susceptibility of multiorbital systems. *Journal of the Physical Society of Japan*, 75(1):013702, 2005.
- [221] MJM Leask, LEJ Roberts, AJ Walter, and WP Wolf. 916. low-temperature magnetic properties of some uranium oxides. *Journal of the Chemical Society (Resumed)*, pages 4788–4794, 1963.
- [222] Edgar F Westrum Jr and Fredrik Grønvold. Low temperature heat capacity and thermodynamic functions of triuranium octoxide. *Journal of the American Chemical Society*, 81(8):1777–1780, 1959.
- [223] Kunihiro Gotoo, Shinzo Nomura, and Keiji Naito. Study on U<sub>4</sub>O<sub>9</sub>—part ii. magnetic susceptibility of U<sub>4</sub>O<sub>9</sub>. *Journal of Physics and Chemistry of Solids*, 26(11):1679–1684, 1965.
- [224] P Erdős, G Solt, A Blaise, JM Fournier, et al. Magnetic susceptibility and the phase transition of NpO<sub>2</sub>. *Physica B+ C*, 102(1-3):164–170, 1980.
- [225] Bruce McCart, GH Lander, and AT Aldred. Structural and magnetic studies of hexagonal β-<sup>242</sup>Pu<sub>2</sub>O<sub>3</sub>. *The Journal of Chemical Physics*, 74(9):5263–5268, 1981.
- [226] DG Karraker. Magnetic susceptibility of BkO<sub>2</sub> in a thorium dioxide matrix. *The Journal of Chemical Physics*, 62(4):1444–1446, 1975.
- [227] DG Karraker. Magnetic susceptibility of <sup>243</sup>AmO<sub>2</sub>. *The Journal of Chemical Physics*, 63(7):3174–3175, 1975.
- [228] David R Lide. *CRC handbook of chemistry and physics*, volume 85. CRC press, 2004.
- [229] Cody A Dennett, Zilong Hua, Amey Khanolkar, Tiankai Yao, Phyllis K Morgan, Timothy A Prusnick, Narayan Poudel, Aaron French, Krzysztof Gofryk, Lingfeng He, et al. The influence of lattice defects, recombination, and clustering on thermal transport in single crystal thorium dioxide. *Apl Materials*, 8(11):111103, 2020.

- [230] Elward T Rodine and Peter L Land. Electronic defect structure of single-crystal  $\text{ThO}_2$  by thermoluminescence. *Physical Review B*, 4(8):2701, 1971.
- [231] Sokrates T Pantelides, Daniel J Mickish, and A Barry Kunz. Electronic structure and properties of magnesium oxide. *Physical Review B*, 10(12):5203, 1974.
- [232] J Belle and RM Berman. Thorium dioxide: properties and nuclear applications. Technical report, USDOE Assistant Secretary for Nuclear Energy, Washington, DC. Office of . . . , 1984.
- [233] P Rodriguez and CV Sundaram. Nuclear and materials aspects of the thorium fuel cycle. *Journal of Nuclear Materials*, 100(1-3):227–249, 1981.
- [234] J-P Dancausse, E Gering, S Heathman, and U Benedict. Pressure-induced phase transition in  $\text{ThO}_2$  and  $\text{PuO}_2$ . *High Pressure Research*, 2(5-6):381–389, 1990.
- [235] A Jayaraman, GA Kourouklis, and LG Van Uitert. A high pressure raman study of  $\text{ThO}_2$  to 40 gpa and pressure-induced phase transition from fluorite structure. *Pramana*, 30(3):225–231, 1988.
- [236] M Idiri, T Le Bihan, S Heathman, and J Rebizant. Behavior of actinide dioxides under pressure:  $\text{UO}_2$  and  $\text{ThO}_2$ . *Physical Review B*, 70(1):014113, 2004.
- [237] U Benedict, GD Andreetti, JM Fournier, and A Wainital. X-ray powder diffraction study of the high pressure behaviour of uranium dioxide. *Journal de Physique Lettres*, 43(6):171–177, 1982.
- [238] Shilpa Singh, Yogesh Sonvane, KA Nekrasov, AS Boyarchenkov, A Ya Kupryazhkin, PN Gajjar, and Sanjeev K Gupta. Systematic investigation of electronic, mechanical and optical properties of  $\text{UO}_2$  at higher pressure: A dft+ u+ soc study. *Solid State Sciences*, 132:106968, 2022.
- [239] Bao-Tian Wang, Ping Zhang, Raquel Lizárraga, Igor Di Marco, and Olle Eriksson. Phonon spectrum, thermodynamic properties, and pressure-temperature phase diagram of uranium dioxide. *Physical Review B*, 88(10):104107, 2013.
- [240] WM Jones, Joseph Gordon, and EA Long. The heat capacities of uranium, uranium trioxide, and uranium dioxide from 15 K to 300 k. *The Journal of Chemical Physics*, 20(4):695–699, 1952.
- [241] Bertram Terence Martin Willis and RI Taylor. Neutron diffraction study of antiferromagnetism in  $\text{UO}_2$ . *Physics Letters*, 17(3):188–190, 1965.
- [242] P Bulet, J Rossat-Mignod, O Vogt, JC Spirlet, J Rebigant, et al. Neutron diffraction on actinides. *Journal of the Less Common Metals*, 121:121–139, 1986.
- [243] G Amoretti, A Blaise, R Caciuffo, JM Fournier, MT Hutchings, R Osborn, and AD Taylor. 5f-electron states in uranium dioxide investigated using high-resolution neutron spectroscopy. *Physical Review B*, 40(3):1856, 1989.
- [244] Elizabeth Blackburn, R Caciuffo, N Magnani, P Santini, PJ Brown, M Enderle, and GH Lander. Spherical neutron spin polarimetry of anisotropic magnetic fluctuations in  $\text{UO}_2$ . *Physical Review B*, 72(18):184411, 2005.
- [245] R Caciuffo, N Magnani, P Santini, S Carretta, G Amoretti, Elizabeth Blackburn, M Enderle, PJ Brown, and GH Lander. Anisotropic magnetic fluctuations in 3-k antiferromagnets. *Journal of magnetism and magnetic materials*, 310(2):1698–1702, 2007.
- [246] Paolo Giannozzi and Paul Erdős. Theoretical analysis of the 3-k magnetic structure and distortion of uranium dioxide. *Journal of magnetism and magnetic materials*, 67(1):75–87, 1987.
- [247] G Dolling and RA Cowley. Observation of magnon-phonon interaction at short wavelengths. *Physical Review Letters*, 16(16):683, 1966.
- [248] RA Cowley and G Dolling. Magnetic excitations in uranium dioxide. *Physical Review*, 167(2):464, 1968.
- [249] M Jaime, A Saul, M Salamon, VS Zapf, N Harrison, T Durakiewicz, JC Lashley, DA Andersson, CR Stanek, JL Smith, et al. Piezomagnetism and magnetoelastic memory in uranium dioxide. *Nature communications*, 8(1):1–7, 2017.
- [250] MS Bryan, JWL Pang, BC Larson, A Chernatynskiy, DL Abernathy, Krzysztof Gofryk, and ME Manley. Impact of anharmonicity on the vibrational entropy and specific heat of  $\text{UO}_2$ . *Physical Review Materials*, 3(6):065405, 2019.
- [251] Denis Gryaznov, Eugene Heifets, and David Sedmidubsky. Density functional theory calculations on magnetic properties of actinide compounds. *Physical Chemistry Chemical Physics*, 12(38):12273–12278, 2010.
- [252] Fei Zhou, Vidvuds Ozoliņš, et al. Crystal field and magnetic structure of  $\text{UO}_2$ . *Physical Review B*, 83(8):085106, 2011.
- [253] Lindsay E Roy, Tomasz Durakiewicz, Richard L Martin, Juan E Peralta, Gustavo E Scuseria, Cliff G Olson, John J Joyce, and Ela Guzewicz. Dispersion in the mott insulator  $\text{UO}_2$ : A comparison of photoemission spectroscopy and screened hybrid density functional theory. *Journal of computational chemistry*, 29(13):2288–2294, 2008.
- [254] Boris Dorado, Michel Freyss, Bernard Amadon, Marjorie Bertolus, Gérald Jomard, and Philippe Garcia. Advances in first-principles modelling of point defects in  $\text{UO}_2$ : f electron correlations and the issue of local energy minima. *Journal of Physics: Condensed Matter*, 25(33):333201, 2013.
- [255] VG Bar'yakhtar, IM Vitebskii, and DA Yablonskii. Magnetoelastic effects in noncollinear antiferromagnets. *Zh. Eksp. Teor. Fiz.*, 89:189–202, 1985.
- [256] JW Ross and DJ Lam. The magnetic susceptibility of neptunium oxide and carbide between 4.2 and 350 k. *Journal of Applied Physics*, 38(3):1451–1453, 1967.
- [257] Darrel W Osborne and Edgar F Westrum Jr. The heat capacity of thorium dioxide from 10 to 305 k. the heat capacity anomalies in uranium dioxide and neptunium dioxide. *The Journal of Chemical Physics*, 21(10):1884–1887, 1953.
- [258] R Caciuffo, GH Lander, JC Spirlet, JM Fournier, and WF Kuhs. A search for anharmonic effects in  $\text{NpO}_2$  at low temperature by neutron diffraction. *Solid state communications*, 64(1):149–152, 1987.
- [259] DE Cox and BC Frazer. A neutron diffraction study of  $\text{NpO}_2$ . *Journal of Physics and Chemistry of Solids*, 28(9):1649–1650, 1967.
- [260] L Heaton, MH Mueller, and JM Williams. A neutron diffraction determination of the coherent scattering amplitude of np and the possible antiferromagnetism of neptunium dioxide. *Journal of Physics and Chemistry of Solids*, 28(9):1651–1654, 1967.
- [261] A Boeuf, R Caciuffo, JM Fournier, L Manes, J Rebizant, F Rustichelli, JC Spirlet, and A Wright. Study of the 25 K  $\text{NpO}_2$  phase transition by a neutron oscillation camera. *Physica Status Solidi Applied Research*, 79(1):K1–

- K3, 1983.
- [262] BD Dunlap, GM Kalvius, DJ Lam, and MB Brodsky. Hyperfine field of  $^{237}\text{Np}$  in  $\text{NpO}_2$ . *Journal of Physics and Chemistry of Solids*, 29(8):1365–1367, 1968.
- [263] JM Friedt, FJ Litterst, and J Rebizant. 25-k phase transition in  $\text{NpO}_2$  from  $\text{Np}^{237}$  Mössbauer spectroscopy. *Physical Review B*, 32(1):257, 1985.
- [264] A Zolnierok, G Solt, and P Erdős. A new approach to the phase transition in  $\text{NpO}_2$ : Model with trivalent Np ions. *Journal of Physics and Chemistry of Solids*, 42(9):773–776, 1981.
- [265] G Amoretti, A Blaise, R Caciuffo, D Di Cola, JM Fournier, MT Hutchings, GH Lander, R Osborn, A Severing, and AD Taylor. Neutron-scattering investigation of the electronic ground state of neptunium dioxide. *Journal of Physics: Condensed Matter*, 4(13):3459, 1992.
- [266] D Mannix, GH Lander, J Rebizant, R Caciuffo, N Bernhoeft, E Lidström, and C Vettier. Unusual magnetism of  $\text{NpO}_2$ : a study with resonant x-ray scattering. *Physical Review B*, 60(22):15187, 1999.
- [267] GM Kalvius, DR Noakes, and O Hartmann.  $\mu\text{sr}$  studies of rare-earth and actinide magnetic materials. *Handbook on the Physics and Chemistry of Rare Earths*, 32:55–451, 2001.
- [268] Ryousuke Shiina, Osamu Sakai, and Hiroyuki Shiba. Magnetic form factor of elastic neutron scattering expected for octupolar phases in  $\text{Ce}_{1-x}\text{La}_x\text{B}_6$  and  $\text{NpO}_2$ . *Journal of the Physical Society of Japan*, 76(9):094702–094702, 2007.
- [269] Ryousuke Shiina. Octupole ordering phases and elastic neutron scattering in  $f$ -electron systems. *Journal of the Physical Society of Japan*, 80(Suppl. B):SB008, 2011.
- [270] JA Paixão, C Detlefs, MJ Longfield, R Caciuffo, P Santini, N Bernhoeft, J Rebizant, and GH Lander. Triple- $q \rightarrow$  octupolar ordering in  $\text{NpO}_2$ . *Physical review letters*, 89(18):187202, 2002.
- [271] M-T Suzuki, Nicola Magnani, and Peter M Oppeneer. First-principles theory of multipolar order in neptunium dioxide. *Physical Review B*, 82(24):241103, 2010.
- [272] RE Walstedt, Y Tokunaga, S Kambe, and H Sakai. Nmr evidence for  $f$ -electron excitations in the multipolar ground state of  $\text{NpO}_2$ . *Physical Review B*, 98(14):144403, 2018.
- [273] Matthias D. Frontzek, Luke R. Sadergaski, Samantha K. Cary, and Binod K. Rai. Search for octupolar ordering in  $\text{NpO}_2$  by unpolarized neutron powder diffraction. *Journal of Solid State*, x(x):x, 2022.
- [274] F De Bruycker, K Boboridis, P Pöml, R Eloirdi, RJM Konings, and D Manara. The melting behaviour of plutonium dioxide: A laser-heating study. *Journal of Nuclear Materials*, 416(1-2):166–172, 2011.
- [275] T Mark McCleskey, Eve Bauer, Quanxi Jia, Anthony K Burrell, Brian L Scott, Steven D Conradson, Alex Mueller, Lindsay Roy, Xiaodong Wen, Gustavo E Scuseria, et al. Optical band gap of  $\text{NpO}_2$  and  $\text{PuO}_2$  from optical absorbance of epitaxial films. *Journal of Applied Physics*, 113(1):013515, 2013.
- [276] N Magnani, P Santini, G Amoretti, and R Caciuffo. Perturbative approach to  $j$  mixing in  $f$ -electron systems: Application to actinide dioxides. *Physical Review B*, 71(5):054405, 2005.
- [277] AB Shick, J Kolorenč, L Havela, T Gouder, and R Caciuffo. Nonmagnetic ground state of  $\text{PuO}_2$ . *Physical Review B*, 89(4):041109, 2014.
- [278] S Kern, RA Robinson, H Nakotte, GH Lander, B Cort, P Watson, and FA Vigil. Crystal-field transition in  $\text{PuO}_2$ . *Physical Review B*, 59(1):104, 1999.
- [279] M Colarieti-Tosti, Olle Eriksson, Lars Nordström, J Wills, and Michael SS Brooks. Crystal-field levels and magnetic susceptibility in  $\text{PuO}_2$ . *Physical Review B*, 65(19):195102, 2002.
- [280] Tsuyoshi Nishi, Masami Nakada, Akinori Itoh, Chikashi Suzuki, Masaru Hirata, and Mitsuo Akabori. Exafs and xanes studies of americium dioxide with fluorite structure. *Journal of nuclear materials*, 374(3):339–343, 2008.
- [281] MM Abraham, LA Boatner, CB Finch, and RW Reynolds. Electron-paramagnetic-resonance investigations of  $5f^5$  configuration ions in cubic single crystals:  $\text{Pu}^{3+}$  in  $\text{ThO}_2$  and  $\text{SrCl}_2$ , and  $\text{Am}^{4+}$  in  $\text{ThO}_2$ . *Physical Review B*, 3(9):2864, 1971.
- [282] W Kolbe, N Edelstein, CB Finch, and MM Abraham. Electron paramagnetic resonance of  $^{239}\text{Pu}^{3+}$  and  $^{243}\text{Am}^{4+}$  in  $\text{CeO}_2$  and of  $^{241}\text{Pu}^{3+}$  in  $\text{ThO}_2$ . *The Journal of Chemical Physics*, 60(2):607–609, 1974.
- [283] Takashi Hotta. Microscopic analysis of multipole susceptibility of actinide dioxides: a scenario of multipole ordering in  $\text{AmO}_2$ . *Physical Review B*, 80(2):024408, 2009.
- [284] M-T Suzuki, Nicola Magnani, and Peter M Oppeneer. Microscopic theory of the insulating electronic ground states of the actinide dioxides  $\text{AnO}_2$  ( $\text{An} = \text{U}, \text{Np}, \text{Pu}, \text{Am}, \text{and Cm}$ ). *Physical Review B*, 88(19):195146, 2013.
- [285] M Matsuura, Y Endoh, H Hiraka, K Yamada, AS Mishchenko, N Nagaosa, and IV Solov'yev. Classical and quantum spin dynamics in the fcc antiferromagnet  $\text{NiS}_2$  with frustration. *Physical Review B*, 68(9):094409, 2003.
- [286] Fumiaki Niikura and Takashi Hotta. Magnetic behavior of curium dioxide with a nonmagnetic ground state. *Physical Review B*, 83(17):172402, 2011.
- [287] Ionut D Prodan, Gustavo E Scuseria, and Richard L Martin. Covalency in the actinide dioxides: Systematic study of the electronic properties using screened hybrid density functional theory. *Physical Review B*, 76(3):033101, 2007.
- [288] Ling Hou, Wei-Dong Li, Fangwei Wang, Olle Eriksson, and Bao-Tian Wang. Structural, electronic, and thermodynamic properties of curium dioxide: Density functional theory calculations. *Physical Review B*, 96(23):235137, 2017.
- [289] AE Putkov, Yu A Teterin, MV Ryzhkov, A Yu Teterin, KI Maslakov, KE Ivanov, SN Kalmykov, and VG Petrov. Electronic structure and nature of chemical bonds in  $\text{BkO}_2$ . *Russian Journal of Physical Chemistry A*, 95(6):1169–1176, 2021.
- [290] LA Boatner and MM Abraham. Electron paramagnetic resonance from actinide elements. *Reports on Progress in Physics*, 41(1):87, 1978.
- [291] N Magnani, G Amoretti, S Carretta, P Santini, and R Caciuffo. Unified crystal-field picture for actinide dioxides. *Journal of Physics and Chemistry of Solids*, 68(11):2020–2023, 2007.
- [292] BW Veal, DJ Lam, H Diamond, and HR Hoekstra. X-ray photoelectron-spectroscopy study of oxides of the transuranium elements Np, Pu, Am, Cm, Bk, and Cf. *Physical Review B*, 15(6):2929, 1977.

- [293] Attila Kovács, Phuong D Dau, Joaquim Marçalo, and John K Gibson. Pentavalent curium, berkelium, and californium in nitrate complexes: Extending actinide chemistry and oxidation states. *Inorganic chemistry*, 57(15):9453–9467, 2018.
- [294] JR Moore, SE Nave, RG Haire, and Paul G Huray. Magnetic susceptibility of californium oxides. *Journal of the Less Common Metals*, 121:187–192, 1986.
- [295] Kingsley Onyebuchi Obodo and Nithaya Chetty. First principles lda+ u and gga+ u study of protactinium and protactinium oxides: dependence on the effective u parameter. *Journal of Physics: Condensed Matter*, 25(14):145603, 2013.
- [296] RP Turcotte, TD Chikalla, and L Eyring. The  $^{248}\text{Cm}$ -oxide system. *Journal of Inorganic and Nuclear Chemistry*, 35(3):809–816, 1973.
- [297] RJM Konings. Thermochemical and thermophysical properties of curium and its oxides. *Journal of nuclear materials*, 298(3):255–268, 2001.
- [298] SJ Rimshaw and EE Ketchen. Curium data sheets. Technical report, Oak Ridge National Lab., Tenn., 1969.
- [299] Martin S Talla Noutack, Grégory Geneste, Gérald Jomard, and Michel Freyss. First-principles investigation of the bulk properties of americium dioxide and sesquioxides. *Physical Review Materials*, 3(3):035001, 2019.
- [300] Tsuyoshi Nishi, Masami Nakada, Chikashi Suzuki, Hiroki Shibata, Akinori Itoh, Mitsuo Akabori, and Masaru Hirata. Local and electronic structure of  $\text{Am}_2\text{O}_3$  and  $\text{AmO}_2$  with xafs spectroscopy. *Journal of nuclear materials*, 401(1-3):138–142, 2010.
- [301] Rudy JM Konings, Ondrej Beneš, Attila Kovács, Dario Manara, David Sedmidubský, Lev Gorokhov, Vladimir S Iorish, Vladimir Yungman, E Shenyavskaya, and E Osina. The thermodynamic properties of the f-elements and their compounds. part 2. the lanthanide and actinide oxides. *Journal of Physical and Chemical Reference Data*, 43(1):013101, 2014.
- [302] Chikashi Suzuki, Tsuyoshi Nishi, Masami Nakada, Mitsuo Akabori, Masaru Hirata, and Yoshiyuki Kaji. Core-hole effect on xanes and electronic structure of minor actinide dioxides with fluorite structure. *Journal of Physics and Chemistry of Solids*, 73(2):209–216, 2012.
- [303] Binod K Rai, AD Christianson, Gabriele Sala, Matthew B Stone, Yaohua Liu, and Andrew F May. Magnetism of  $\text{Nd}_2\text{O}_3$  single crystals near the néel temperature. *Physical Review B*, 102(5):054434, 2020.
- [304] Gabriele Sala, Matthew B Stone, Binod K Rai, Andrew F May, CR Dela Cruz, H Suriya Arachchige, Georg Ehlers, Victor R Fanelli, Vasile O Garlea, Mark D Lumsden, et al. Physical properties of the trigonal binary compound  $\text{Nd}_2\text{O}_3$ . *Physical Review Materials*, 2(11):114407, 2018.
- [305] M Wulff and GH Lander. Magnetic structure and pu ground state in  $\beta\text{-Pu}_2\text{O}_3$ . *The Journal of chemical physics*, 89(5):3295–3299, 1988.
- [306] Yong Lu, Yu Yang, Fawei Zheng, and Ping Zhang. Electronic and thermodynamic properties of  $\alpha\text{-Pu}_2\text{O}_3$ . *Physics Letters A*, 378(41):3060–3065, 2014.
- [307] Marco Molinari, Nicholas A Brincat, Geoffrey C Allen, and Stephen C Parker. Structure and properties of some layered  $\text{U}_2\text{O}_5$  phases: A density functional theory study. *Inorganic chemistry*, 56(8):4468–4473, 2017.
- [308] Nicholas A Brincat, Stephen C Parker, Marco Molinari, Geoffrey C Allen, and Mark T Storr. Density functional theory investigation of the layered uranium oxides  $\text{U}_3\text{O}_8$  and  $\text{U}_2\text{O}_5$ . *Dalton Transactions*, 44(6):2613–2622, 2015.
- [309] DA Andersson, Gianguido Baldinozzi, Lionel Desgranges, DR Conradson, and SD Conradson. Density functional theory calculations of  $\text{UO}_2$  oxidation: Evolution of  $\text{UO}_{2+x}$ ,  $\text{U}_4\text{O}_{9-y}$ ,  $\text{U}_3\text{O}_7$ , and  $\text{U}_3\text{O}_8$ . *Inorganic chemistry*, 52(5):2769–2778, 2013.
- [310] Y Yun, Jan Ruzs, M-T Suzuki, and PM Oppeneer. First-principles investigation of higher oxides of uranium and neptunium:  $\text{U}_3\text{O}_8$  and  $\text{Np}_2\text{O}_5$ . *Physical Review B*, 83(7):075109, 2011.
- [311] Lei Zhang, Ewa A Dzik, Ginger E Sigmon, Jennifer ES Szymanowski, Alexandra Navrotsky, and Peter C Burns. Experimental thermochemistry of neptunium oxides:  $\text{Np}_2\text{O}_5$  and  $\text{NpO}_2$ . *Journal of Nuclear Materials*, 501:398–403, 2018.
- [312] Sara B Isbill, Ashley E Shields, Jennifer L Niedziela, and Andrew J Miskowiec. Density functional theory investigations into the magnetic ordering of  $\text{U}_3\text{O}_8$ . *Physical Review Materials*, 6(10):104409, 2022.
- [313] Pascal Naubereit, Tina Gottwald, Dominik Studer, and Klaus Wendt. Excited atomic energy levels in protactinium by resonance ionization spectroscopy. *Physical Review A*, 98(2):022505, 2018.
- [314] RJ Ackermann, AT Chang, and Charles A Sorrell. Thermal expansion and phase transformations of the  $\text{U}_3\text{O}_{8-z}$  phase in air. *Journal of Inorganic and Nuclear Chemistry*, 39(1):75–85, 1977.
- [315] Stanley Siegel. The crystal structure of trigonal  $\text{U}_3\text{O}_8$ . *Acta Crystallographica*, 8(10):617–619, 1955.
- [316] Andrew Miskowiec, Tyler Spano, Zach E Brubaker, JL Niedziela, DL Abernathy, Rodney D Hunt, and Sarah Finkeldei. Antiferromagnetic ordering and possible lattice response to dynamic uranium valence in  $\text{U}_3\text{O}_8$ . *Physical Review B*, 103(20):205101, 2021.
- [317] Xiao-Dong Wen, Richard L Martin, Gustavo E Scuseria, Sven P Rudin, Enrique R Batista, and Anthony K Burrell. Screened hybrid and dft+ u studies of the structural, electronic, and optical properties of  $\text{U}_3\text{O}_8$ . *Journal of Physics: Condensed Matter*, 25(2):025501, 2012.
- [318] NC Popa and BTM Willis.  $\text{U}_4\text{O}_9$ : atoms in general sites giving the hkl extinctions of special sites. *Acta Crystallographica Section A: Foundations of Crystallography*, 60(4):318–321, 2004.
- [319] RI Cooper and BTM Willis. Refinement of the structure of  $\beta\text{-U}_4\text{O}_9$ . *Acta Crystallographica Section A: Foundations of Crystallography*, 60(4):322–325, 2004.
- [320] KO Kvashnina, Sergei M Butorin, P Martin, and P Glatzel. Chemical state of complex uranium oxides. *Physical review letters*, 111(25):253002, 2013.
- [321] Lionel Desgranges, G Baldinozzi, Patrick Simon, G Guimbretière, and A Canizares. Raman spectrum of  $\text{U}_4\text{O}_9$ : a new interpretation of damage lines in  $\text{UO}_2$ . *Journal of Raman Spectroscopy*, 43(3):455–458, 2012.
- [322] F Garrido, AC Hannon, RM Ibberson, L Nowicki, and BTM Willis. Neutron diffraction studies of  $\text{U}_4\text{O}_9$ : Comparison with exafs results. *Inorganic chemistry*, 45(20):8408–8413, 2006.
- [323] Gregory Leinders, René Bes, Janne Pakarinen, Kristina Kvashnina, and Marc Verwerft. Evolution of the uranium chemical state in mixed-valence oxides. *Inorganic chemistry*, 56(12):6784–6787, 2017.

- [324] Howard E Flotow, Darrell W Osborne, and Edgar F Westrum Jr. Heat capacity of tetrauranium ennea-oxide ( $U_4O_9$ ) from 1.6° to 24° k. the magnetic contribution to the entropy. *The Journal of Chemical Physics*, 49(5):2438–2442, 1968.
- [325] G Rousseau, L Desgranges, F Charlot, N Mil- lot, JC Nièpce, M Pijolat, F Valdivieso, Gianguido Baldinozzi, and JF Béarar. A detailed study of  $UO_2$  to  $U_3O_8$  oxidation phases and the associated rate-limiting steps. *Journal of nuclear materials*, 355(1-3):10–20, 2006.
- [326] Nicholas A Brincat, M Molinari, Geoffrey C Allen, Mark T Storr, and Stephen C Parker. Density func- tional theory calculations of defective  $UO_2$  at  $U_3O_7$  sto- ichiometry. *Journal of Nuclear Materials*, 467:724–729, 2015.
- [327] Kaushik Sanyal, Ajay Khooha, Gangadhar Das, MK Ti- wari, and NL Misra. Direct determination of oxidation states of uranium in mixed-valent uranium oxides using total reflection x-ray fluorescence x-ray absorption near- edge spectroscopy. *Analytical chemistry*, 89(1):871–876, 2017.
- [328] Gregory Leinders, Gianguido Baldinozzi, Clemens Rit- ter, Rolando Saniz, Ine Arts, Dirk Lamoen, and Marc Verwerft. Charge localization and magnetic correlations in the refined structure of  $U_3O_7$ . *Inorganic Chemistry*, 60(14):10550–10564, 2021.
- [329] Erich Heinz Pieter Cordfunke and P Aling. System  $UO_3 + U_3O_8$ : dissociation pressure of  $\gamma$ - $UO_3$ . *Transactions of the Faraday Society*, 61:50–53, 1965.
- [330] EHP Cordfunke and Edgar F Westrum Jr. The thermo- dynamic properties of  $\beta$ - $UO_3$  and  $\gamma$ - $UO_3$ . *Thermochim- ica acta*, 124:285–296, 1988.
- [331] Jiang-Jiang Ma, Cheng-Bin Zhang, Ruizhi Qiu, Ping Zhang, Bingyun Ao, and Bao-Tian Wang. Pressure- induced structural and electronic phase transitions of uranium trioxide. *Physical Review B*, 104(17):174103, 2021.
- [332] Bingyun Ao, Ruizhi Qiu, Jun Tang, and Jinfan Chen. New theoretical insights into the actual oxidation states of uranium in the solid-state compounds. *Journal of Nuclear Materials*, 543:152563, 2021.
- [333] Nicholas A Brincat, Stephen C Parker, Marco Moli- nari, Geoffrey C Allen, and Mark T Storr. Ab initio investigation of the  $UO_3$  polymorphs: Structural prop- erties and thermodynamic stability. *Inorganic Chem- istry*, 53(23):12253–12264, 2014.
- [334] L Casillas-Trujillo, G Baldinozzi, MK Patel, H Xu, and KE Sickafus. Comparison of bonding and charge den- sity in  $\delta$ - $UO_3$ ,  $\gamma$ - $UO_3$ , and  $La_6UO_{12}$ . *Physical Review Materials*, 1(6):065404, 2017.